Εθνικό Μετσόβιο Πολυτεχνείο
Σχολή Πολιτικών Μηχανικών
Τομέας Γεωτεχνικής

National Technical University of Athens
School of Civil Engineering
Geotechnical Division

Διπλωματική Εργασία

Παπαδόπουλος Ευθύμιος

Επιβλέποντες :

Καθηγητής Γ. Γκαζέτας

Δρ. Ι. Αναστασόπουλος

ΜΕΤΑΠΛΑΣΤΙΚΗ ΛΙΚΝΙΣΤΙΚΗ ΑΠΟΚΡΙΣΗ ΜΟΝΟΒΑΘΜΙΟΥ ΤΑΛΑΝΤΩΤΗ: ΠΕΙΡΑΜΑΤΙΚΗ ΔΙΕΡΕΥΝΗΣΗ

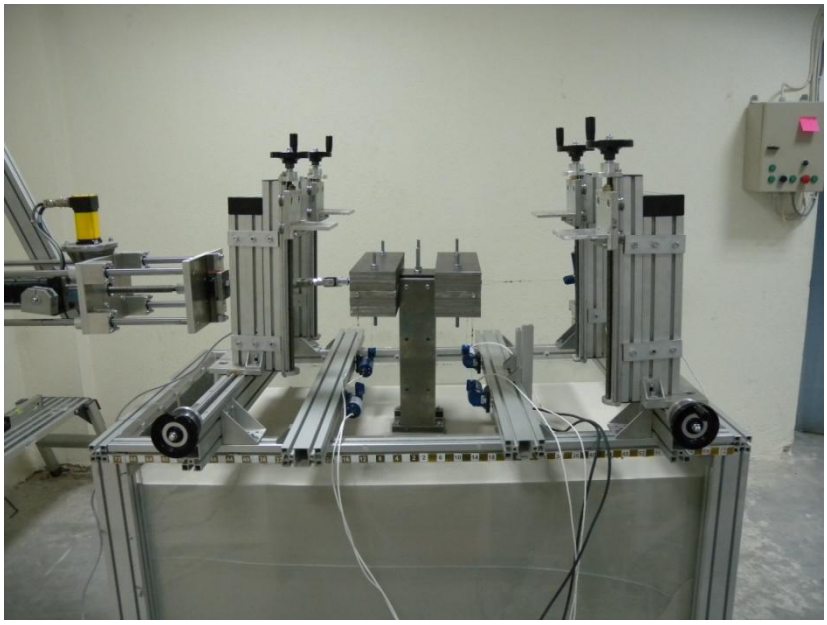

METAPLASTIC ROCKING RESPONSE OF 1-DoF SYSTEM : EXPERIMENTAL INVESTIGATION

Diploma Thesis

PAPADOPOULOS EFTHYMIOS

Supervised by :

Professor G.Gazetas

Dr. I. Anastasopoulos

ΑΘΗΝΑ ΙΟΥΝΙΟΣ 2011

ATHENS JUNE 2011

Acknowledgements

Having reached the end of my undergraduate journey, I would like to express my deepest gratitude to all the people that helped me during the course of this journey.

Special thanks should be attributed to the Director of the Laboratory of soil Mechanics of the National Technical University of Athens, Professor George Gazetas, for the continuous interest he showed in this work as well as inspiring and influencing me in the first place to pursue this goal.

Specifically, for the duration of this thesis, I would like to thank Dr. Ioannis Anastasopoulos, Rallis Kourkoulis, Fani Gelagoti and everyone else in the laboratory for their precious help and counsel. Without them, this piece of work would not have been realized.

I would also like to thank my colleagues and fellow researchers Aggelos Tsatsis and Giota Kokkali, for their support in conducting the experiments and constantly advising and supporting me in any problems I encountered.

Last but not least, I would like to thank my family, my friends and relatives, and every single person who helped shape my personality.

Dedicated to my cousin Nana

Table of Contents

CHAPTER I:

INTRODUCTION

1.1 Current Earthquake Design Principles

For the last 30 or so years the scientific community of earthquake engineering has focused on studying ways to alleviate the destruction caused by large earthquakes that greatly exceed the ones expected by design standards. In these cases, inelastic behavior of the structure cannot be averted. To this end, structures are designed so that failure is guided to the least important, in terms of structural integrity, elements and brittle failure mechanisms are not mobilized.

While inelastic response of the superstructure is allowed for the cases of strong earthquake shaking, current seismic design principles and regional Codes, like EC8 or FEMA guidelines, do not take advantage of strength and ductility available on the soil-foundation level imposing elastic foundation response. This approach derives from the fact that inspection and repair of damaged soil-foundation systems might be a rather difficult and controversial task. Hence, prospective designers must ensure that the soil-foundation system will operate in a region far away from failure. To this end, many thresholds and safety measures are imposed: mobilisation of soil bearing-

capacity, foundation uplifting, sliding, or any combination of the above are forbidden or strictly limited. This is achieved by imposing over-strength factors and conservative factors of safety against all such possible "failure" modes. As a result, increased ductility requirements on structural elements are required.

1.2 Inelastic Foundation Response : A new pioneering approach

Experience gained from past earthquake events has proved that, on many occasions seismic shaking is so strong that even these safety valves cannot guarantee the desired behaviour and the safety of the structure. Fortunately though, and contrary to common belief, recent studies *(Paolucci 1997; Pecker, 1998, 2003; FEMA 356; Gazetas et al, 2003)* have shown that allowing non-linear soil-foundation response of the above types can have a beneficial role in the overall response of the structure in various ways. Due to the cyclic and kinematic nature of seismic shaking, such response does not necessarily constitute "failure". In addition to that, nonlinearity of the soil-foundation system can act as a fuse mechanism, dissipating earthquake energy and potentially reducing demands exerted on the structural components of the building (*Gajan et al., 2005*).

In this framework, recent studies have been conducted, investigating the soil-foundation system's non-linear response on an analytical, numerical and

experimental basis under strong earthquake shaking. The response of simple 1-dof systems that are assumed to be founded on isolated footings lying on inelastic soil has been mainly explored. These studies strive to take into account as realistically as possible the nonlinear soil-foundation system's response, emanating mainly from geometric nonlinearities such as foundation sliding or uplift, as well as material inelasticity, i.e., soil plastification.

This response has been investigated by means of : (i) sophisticated Winkler based models that simultaneously capture the settlement-rotation at the base of the footing (*Yim and Chopra, 1985; Nakaki and Hart, 1987; Chen and Lai; 2003*; *Houlsby et al., 2005*; *Allotey and Naggar, 2003, 2007; Raychowdhury and Hutchinson, 2009)*; (ii) advanced macro-elements models where the entire soil-foundation system is replaced by one single element that describes the generalized force-displacement behavior of a point (normally at the center of the footing) in the vertical, horizontal and rotational dimensions and (*Nova & Montrasio, 1991; Paolucci, 1997*; *Pedretti, 1998; Le Pape and Sieffert, 2001; Crémer, 2001; Crémer et al, 2001; Grange et al, 2008*; *Chatzigogos et al, 2009, 2010*) (iii) direct methods (i.e. finite elements or finite difference algorithms) where both the structure and the foundation-soil system are modeled together through an assemblage of finite elements (*Tan, 1990; Butterfield and Gottardi, 1995; Taiebat and Carter, 2000 ; Gourvenec 2007; Anastasopoulos et al , 2010, 2011*).

The above methods have been applied to various studies. The results have shown that allowing this kind of behavior to take place acts as an energy

dissipation mechanism that limits the seismic stresses exerted on the components of the superstructure, thus providing substantially large safety margins even for seismic motions that exceed the design limits. These findings have been further verified by numerous experimental results —centrifuge, large scale and 1-g reduced scale tests— (*Faccioli et al., 2001; Kutter et al., 2003; Gajan et al, 2005; Kawashima et al., 2007; Drosos et al. 2010(?)*).

A "new design philosophy" has been introduced by Anastasopoulos et al. (2010), for a simple single degree of freedom system, representative of a single pier of a bridge on surface foundation.. The concept behind this approach is the intention under-design of the foundation , an approach totally in contrast to common practice. In this way, failure is guided to the soil-foundation system instead of the structural elements providing larger safety margins towards collapse. However, increased settlement is the price to pay. This concept has been further investigated for frame structures on isolated surface footings by Gelagoti et al [2011].

1.3 Metaplastic Rocking Response of 1-dof Systems

For the case of simple 1-dof systems lying on inelastic surface, there are several parameters relating to the nonlinear response, geometrical, as well as material. The slenderness of the foundation-superstructure system (i.e. geometrical characteristics and specifically the height to foundation width ratio (aspect ratio = h/B) determines the rocking behavior. Whereas slender structures tend to uplift from the supporting soil even for small amplitudes of earthquake shaking, short ones tend to maintain contact with their base and

respond by sliding on the soil-foundation interface. Moreover, slender structures are especially vulnerable to moment loading and second order effects play a dominant role in their response, while short ones suffer from shear force loading. Regarding structural vertical loads, the factor of safety against vertical load FS_v controls the interplay between uplifting *or* soil yielding. Soil properties and structural flexibility also play an important role and should be accounted for in order to investigate the metaplastic rocking response of 1-dof systems.

1.4 Uncertainties and Limitations

Unfortunately, there are uncertainties that prevent us from being able to accurately predict this kind of response and limitations regarding the applications of such a concept to design methodology. Large residual displacements (settlement and sliding) and rotations, unacceptable for current seismic design, pose a definite problem. Furthermore, there remains a chance that the building overturns even more easily than when we allow only elastic response of the soil-foundation system.

Another problem is that soil is a very heterogeneous material and soil properties are not or cannot be always closely measured or estimated. Foundation rocking is a mechanism that, as mentioned before, depends to a large extent on the soil properties as to the nature of the systems response. A governing factor regarding foundation rocking is the Factor of safety against

vertical loading FS_v. Low FS_v results in so called sinking dominated behaviour, mainly mobilizing soil bearing capacity and resulting in high residual settlement values. High FS_v results in uplift-dominated behaviour. Knowing the FS_v involves knowing the soil properties.

1.5 Shallow Soil Improvement

These problems pose restrains to the concept being fully implemented in design philosophy and codes. In an effort to overcome this obstacle, the concept of shallow soil improvement was introduced. Generally in geotechnical engineering, soil improvement has been implemented in several problems, as a way to increase soil strength and reduce settlement derived from vertical loads.

The reason shallow soil improvement is considered as a remedy to the problems associated with foundation rocking is because of the “shallow” nature if this phenomenon. Foundation rocking affects mainly the upper levels of the soil stratum, so these are the ones that dictate the behaviour of the system. Improving the soil by replacing the upper levels of the stratum with a “crust” of the desired – and more easily controllable – soil properties could give designers the opportunity to choose the way the foundation reacts to strong shaking, according to the superstructure’s needs and other requirements. Being able to accurately control and predict the response of the structure is a step closer to this concept being implemented in design codes and common practice.

1.6 Scope of this work

This piece of work attempts to shed some more light to the idea of foundation rocking and more specifically controlling this behaviour through shallow soil improvement. To this end, a series of horizontal monotonic and slow cyclic pushover tests were conducted in the laboratory of soil mechanics of the National Technical University of Athens (NTUA). In detail, this diploma thesis will investigate:

- The Monotonic and slow cyclic loading of structures well beyond their elastic behaviour threshold.
- The effect of the vertical factor of safety FS_v on the rocking response of the construction, either by comparing the same construction lying on different soil strata, or different structures lying on the same soil deposit.
- The response of structures of the same FS_v, achieved by placing different structures on different soil strata.
- The response of the same structure subjected to different loading protocols.
- The effect of shallow soil improvement stretching to various depths on the response of the structure. This will be done for various structures that one would initially predict different behaviour for each.

CHAPTER II:

Problem Definition and Methodology

2.1 Problem definition

Slender structures, such as bridge piers and multi storey buildings, are subjected to combined loading during earthquake shaking. The moment developed at the foundation level plays a dominant role in the behavior of these systems defining the inertia transmitted to the superstructure. Several researchers have observed that foundation uplifting as well as mobilization of soil bearing capacity can have a beneficial effect on the response of these systems, resulting in significant energy dissipation and limiting the distress of the superstructure (Gajan et al, 2005).

Several parameters are related to the nonlinear response of simple single degree of freedom systems lying on surface foundations. The slenderness of the system (i.e. geometrical characteristics) determines the uplifting behavior, whereas the factor of safety against vertical load controls the interplay between uplifting *and* soil yielding. Moreover, soil properties should be accurately estimated in order to describe the metaplastic response of 1-dof systems.

However, this is not always feasible, due to the inherent soil heterogeneity and the lack of geotechnical data.

In an attempt to illuminate the metaplastic response of 1-dof systems and highlight the key-response parameters of the problem, a series of 1g reduced scale experiments were conducted at the Laboratory of Soil Mechanics of the National Technical University of Athens (NTUA). . Systems with varying factors of safety against vertical loading were subjected to monotonic and slow cyclic loading. Homogeneous and two-layered soil deposits were examined, in order to explore the effectiveness of the concept of shallow soil improvement. Different cyclic load protocols were applied to the systems in order to capture their inelastic response under horizontal loading of varying displacement amplitudes. The Table at the end of the chapter shows a complete list of all the experiments conducted.

The single degree of freedom system investigated is representative of a relatively slender bridge pier, supported on surface square foundation. Unless otherwise noted, all mentioned dimensions hereafter refer to in model scale.

2.2 Experimental Set-Up

Sandbox

For the purposes of this series of experiments, dry Longstone, an industrially produced and uniform quartz sand was used. The parameters of this sand are D_{50} = 0.15mm and C_u = 1.42. The void ratios were measured to be e_{max} = 0.995 and e_{min} =0.614 and the specific solids weight G_s = 2.64. The sand was layered using dry pluviation on a rigid container with dimensions of 160 x 90 x 75 cm. Adjusting the speed and the height of the pluviation, as well as the aperture of the soil hopper enables us to produce soil samples of the desired relative density D_r. The Chart at the end of the chapter shows the pluviation results of the Longstone sand and the marked dots display the setup used to create the soil samples.

The barriers of the box are transparent and are made of glass on the inside and Plexiglas on the outside. The Plexiglas is used in order to achieve the desired rigidity and durability, whereas the glass protects against scratching and minimizes friction.

At this point, it is noted that the stress field in the supporting soil cannot be correctly reproduced in reduced–scale testing. This is presumed to be the main shortcoming of small scale testing, which is alleviated by centrifuge model testing. The significantly lower levels of effective stress in the model result in overestimating φ' , and as a result the soil appears to have larger strength and dilatancy, in comparison to the real scale prototype. Nevertheless, 1 g shaking

table testing is a valid method, provided that such scale effects and the stress-dependent soil behavior are accounted for in the design of the experiments and results are interpreted appropriately.

Model

The foundation–superstructure model used in this series of experiments consists of a square foundation of dimensions 15 cm x 15 cm x 2 cm, two rigid columns of height 45 cm and a slab located 45 cm above the foundation level. The superstructure mass is placed symmetrically above and below the slab level so as the center of mass remains the same for all cases examined. Consequently, the aspect ratio of the system yields h/B = 3. Figure** portrays the complete model and provides a detailed description of all the model parts, including dimensions and material type. Sandpaper was placed under the foundation in order to achieve the desired friction.

Pushover apparatus and Instrumentation

The desired horizontal displacement at the mass level is applied through a pushover apparatus consisting of a servomotor attached to a screw-jack actuator. This device is controlled by a computer, through which the parameters of the loading pack, including the desired displacement, velocity and acceleration can be adjusted. The applied load is measured through a load

cell of maximum capacity of 200 kg which is attached to the actuator. The pushover apparatus is rigidly attached to the wall. The other point of the device is connected to the foundation-superstructure model using a pin and clevis attachment enabling the system to freely settle, slide and rotate as horizontal load is applied. A linear guideway is inserted between the actuator and the servomotor. In this way, the model is exclusively subjected to horizontal loading at the mass level and parasitical loading is avoided even in the case of large imposed displacements. The Pushover apparatus is illustrated at the end of the chapter.

In order to capture the displacements of the foundation and the superstructure a combined system of wire and laser transducers was implemented. Laser transducers were placed on the foundation level in order to capture sliding and potential out of plane rotation. Wire transducers were attached vertically on the four ends of the superstructure mass in order to measure vertical displacements. One wired transducer was also placed horizontally at the mass level to measure the horizontal displacement. A complete setup of the instrumentation is presented at the end of the chapter.

Load protocol

The systems were subjected to monotonic and slow cyclic horizontal loading. Since the displacement amplitude and the sequence of horizontal loading plays a vital role in the behavior of the foundation, three different types

of cyclic load protocols were adopted in the series of experiments.. Type I, the primary load protocol, consists of 14 cycles of increasing displacement, ranging from 2mm to 40mm. Type II consists of 7 cycles of increasing amplitude ranging from 4mm to 40mm. Type III consists of 31 cycles, divided into 10 cycles of 4mm, 10 cycles of 8mm, 5 cycles of 16mm, 3 cycles of 24mm and 3 cycles of 40mm, in increasing order. For all load types, the displacement was imposed in load packs in order to achieve the desired speed and avoid any dynamic effects. Illustrations of the Load Protocols are displayed at the end of the chapter.

Model Preparation

The preparation for the test begins with the layering of the sand in the box. The height of the soil deposit ranges from 50 to 55 cm. After sand layering is completed, the model is placed on four jacks attached to the sandbox which enable us to place the model on the desired position both horizontally and vertically. Due to the heavy weight of the system, this is achieved using a crane bridge. Once the model has been placed on the jacks, the sandbox is moved to the prescribed location for the test. Then the model is carefully lowered to touch the soil. To monitor this procedure, electronic spirit levels are placed on the superstructure to certify that the foundation is placed parallel to the soil surface, with no inclination. Once this is completed, the instruments mentioned above are installed and connected to the recording system.

After checking that all the measurement instruments are working properly, the load protocol is uploaded to the control computer and the test begins. Each cyclic test consists of 1 to 5 load packs whereas the monotonic test consists of a single load pack. Initial and final measurements are taken before and after each load pack, respectively regarding the force displayed on the load cell and the foundation inclination, for verification purposes.

At the end of the test, the model is removed carefully from the sand using the aforementioned jacks, to preserve the area underneath as well as the failure surface undisturbed. The box is then emptied to be ready for the next experiment.

2.3 Data Acquisition and Processing

In order to process the data collected throughout the test, all instruments are connected to a mainframe computer, where data is recorded using sophisticated software. The data is then saved and processed. First, the saved data goes through a filtering process in MATLAB code. Unwanted recordings are erased and the load packs are merged into a single file for the case of cyclic pushover tests. The output is smoothened in order to eliminate the “noise” produced by the instruments due to the small range of displacements compared to their capacity or the electrical current. Then, the new file is inserted into a Microsoft Excel spreadsheet where the response curves are derived.

2.4 Vertical Pushdown Tests

The safety factor against vertical load is a parameter that dictates to a great extent the behavior of structures during earthquake shaking. In order to achieve the desired FS_v, the bearing capacity of the soil-foundation system should be known. To this end, a series of experiments was conducted, involving vertical monotonic and cyclic pushdown tests on various square footings lying on different types of sand, including soil deposits with shallow improvement. The full description and the results of these tests can be found in the respective report (LSM., 2011a). The vertical load capacity of systems with foundation width B = 0.15 m is used herein, in order to calculate the required FS_v. A Table at the end of the chapter summarizes the capacity for all soil types investigated in this series.

FIGURES

Date	Experiment	Description of experiment		
		Footing width	Soil	Type of vertical loading
25/1/2011	**7**	*0.15 m*	Dense sand	Central monotonic
				Central cyclic
26/1/2011	**8**	*0.15 m*	Dense sand	Central monotonic
27/1/2011	**9**	*0.15 m*	Dense sand	Central cyclic
31/1/2011	**10**	*0.15 m*	Sand of medium density	Central monotonic
1/2/2011	**11**	*0.15 m*	Sand of medium density	Central cyclic
2/2/2011	**12**	*0.25 m*	Sand of medium density	Eccentric monotonic
3/2/2011	**13**	*0.25 m*	Sand of medium density	Eccentric monotonic
7/2/2011	**14**	*0.25 m*	Sand of medium density	Central monotonic
8/2/2011	**15**	*0.25 m*	Sand of medium density	Central cyclic
10/2/2011	**17**	*0.25 m*	Dense sand	Eccentric monotonic
11/2/2011	**18**	*0.25 m*	Dense sand	Eccentric monotonic
23/2/2011	**22**	*0.15 m*	Two Layered Soil **(z/B = 1)**	Central monotonic
24/2/2011	**23**	*0.15 m*	Two Layered Soil **(z/B = 1)**	Central cyclic
25/2/2011	**24**	*0.15 m*	Two Layered Soil **(z/B = 0.5)**	Central monotonic
1/3/2011	**26**	*0.15 m*	Two Layered Soil **(z/B = 0.5)**	Central cyclic
2/3/2011	**27**	*0.15 m*	Two Layered Soil **(z/B = 0.25)**	Central cyclic
3/3/2011	**28**	*0.15 m*	Two Layered Soil **(z/B = 0.25)**	Central monotonic
4/3/2011	**29**	*0.15 m*	Loose sand	Central monotonic
8/3/2011	**30**	*0.15 m*	Two Layered Soil **(z/B = 0.5)**	Central monotonic
10/3/2011	**31**	*0.15 m*	Two Layered Soil **(z/B = 1)**	Central monotonic
11/3/2011	**32**	*0.15 m*	Two Layered Soil **(z/B = 0.25)**	Central monotonic

Timetable of the full series of experiments conducted.

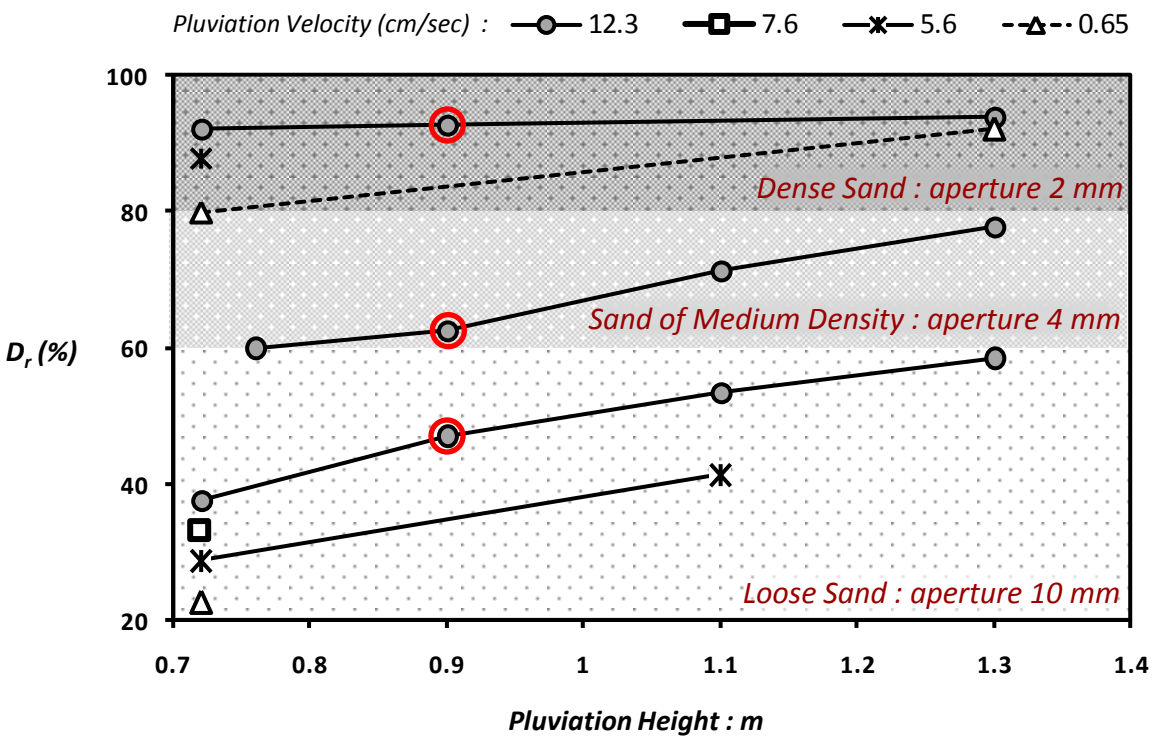

Pluviation Results for the Longstone sand. The red dots represent the Sand Densities used in the experiments.

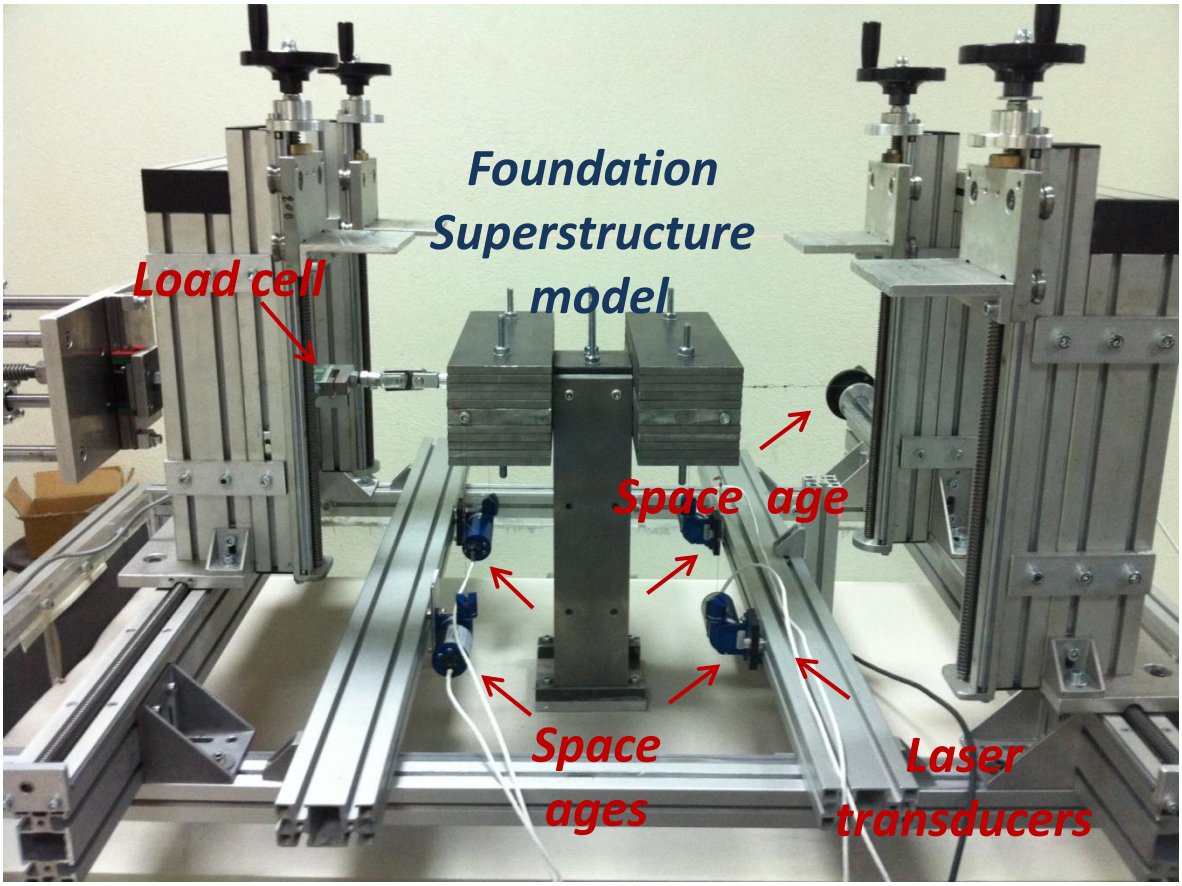

Pushover apparatus and instrumentation view

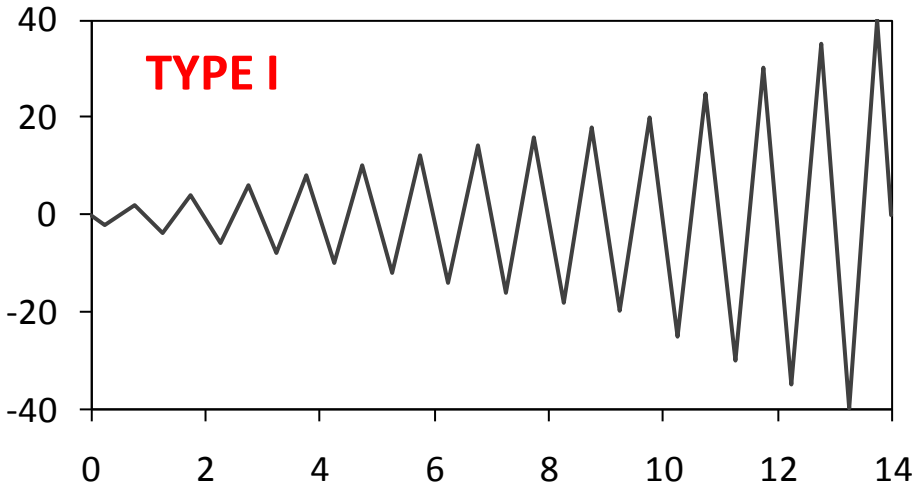

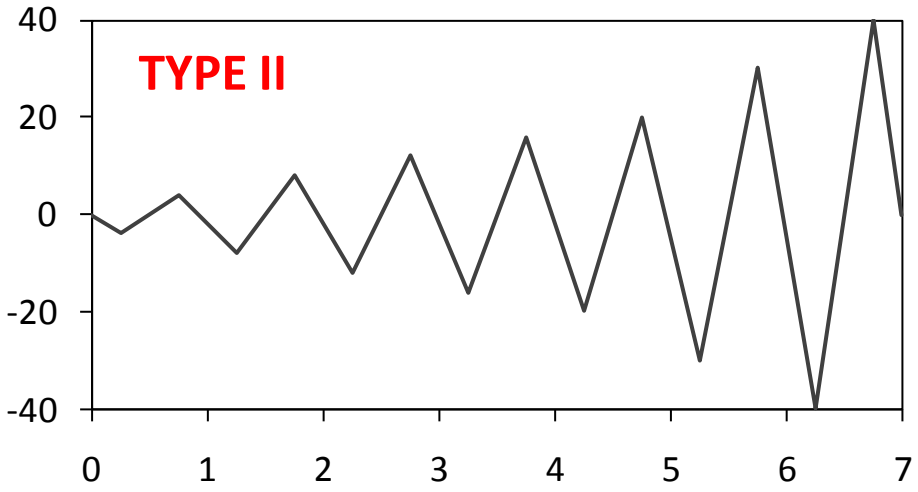

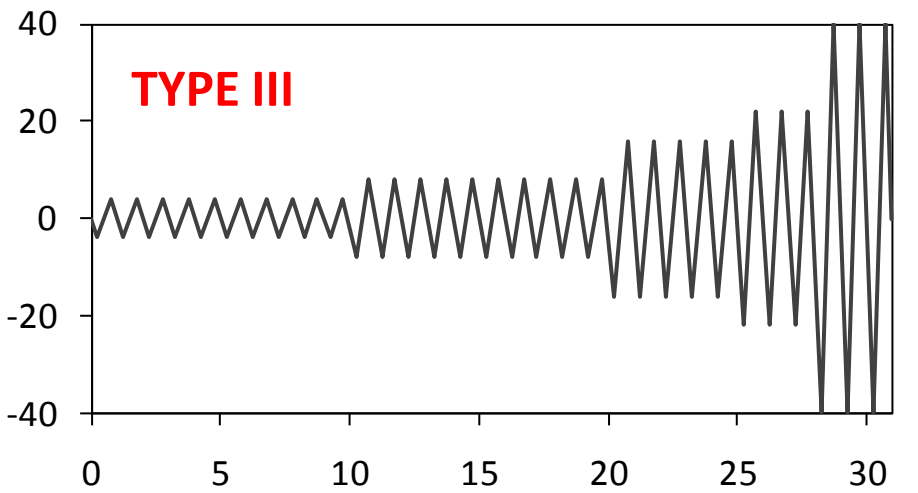

Time history illustration of the Load protocols used in the experiments.

Homogeneous soil:

Dense sand (Dr=93%)							
	Nult=	4.83	kN	=>	Nult=	492.4	kg
Sand of medium density (Dr=65%)							
	Nult=	2.48	kN	=>	Nult=	252.8	kg
Loose sand (Dr=45%)							
	Nult=	1.7	kN	=>	Nult=	173.3	kg

Two layered soil:

Improvement of sand of medium density:

z/B=1							
	Nult=	3.96	kN	=>	Nult=	403.7	kg
z/B=0.5							
	Nult=	3.03	kN	=>	Nult=	308.9	kg
z/B=0.25							
	Nult=	2.73	kN	=>	Nult=	278.3	kg

Improvement of loose sand:

z/B=1							
	Nult=	3.4	kN	=>	Nult=	346.6	kg
z/B=0.5							
	Nult=	2.45	kN	=>	Nult=	249.7	kg
z/B=0.25							
	Nult=	1.95	kN	=>	Nult=	198.8	kg

Table showing the Vertical bearing Capacity for each soil Deposit, calculated from Vertical Pushdown Tests.

CHAPTER III :

Investigation on Homogeneous Soil Profiles

3.1 Introduction

The basic parameters investigated are shown in **Figure 3.1**. Three structures based on the same foundation were selected, differing in the superstructure mass. The structures were on three different types of sand with differing relative density. The parameters we selected so that the different systems demonstrate distinctly different behaviors, from strictly uplift-dominated response to strictly sinking response.

Some of the results extracted were compared to Large Shaking table experiments that took place at Public Works Research Institute (PWRI) Tsukuba, Japan, to validate the results.

3.2 The Effect of FS_v

3.2.1 Same soil (dense)-different mass

Monotonic Loading

To begin with, slow monotonic horizontal tests were conducted. In this case three different superstructures each with a mass of 35kg, 70kg and 100kg, lying on dense sand were tested. The results in terms Of M: θ and w: θ are shown in **Figure 3.2**.

In the w: θ chart, it can be observed that there are three distinct responses in terms of rocking. The lightweight model displays a dominantly uplifting response with a very small range of angle where sinking is noticed. The opposite can be said for the heavy structure, which displays settlement for a wide range of θ. This should be mainly attributed to soil yielding underneath the foundation. For the moderate weight model, we can say that its response lies somewhere between the two, but still closer to the light one.

Next a comparison between the models is made in terms of Moment-Rotation. As far as ultimate moment is concerned, we can see that the heavier the foundation, the larger bearing capacity is displayed. This is in accordance

to the results derived from the various failure envelopes found in literature (Butterfield and Gottardi, 1995; Gourvenec, 2004) where maximum moment capacity is observed for FS_v in the order of 2. In terms of $\theta_{u,}$ it can be evidently observed that the larger the safety factor against vertical loading, the more the θ_u measured approaches the value expected for 1-dof systems founded on rigid base, given by the following formula :

$$\theta c = \tan^{-1}\frac{B}{2H}.$$

This is something to be expected, because as the structure gets lighter, less soil deformations are observed and the stresses under the part of the foundation that rotates do not cause soil failure as easily.

An effort was made to calculate rotational stiffness with increasing rotation. This is demonstrated in the last chart. Rotational stiffness is tied to the shear modulus G, which for sands is relative to the confinement stresses. For reduced scale experiments, confinement stresses are mostly attributed to the surcharge imposed by the superstructure. Thus, the heavy footing demonstrates a much larger rotational stiffness.

For monotonic loading, the maximum moment achieved was compared to the failure envelopes proposed by Butterfield and Gottardi (1995). In **Figure 3.3**, one can notice moderate differences between the Horizontal load calculated by the failure envelopes and the one measured during the tests, especially for the lightweight model. This is unfortunately one of the flaws of

reduced scale experiments, due to the fact that soil deformations are governed strictly by the surcharge, because of the small geostatic stresses. The friction angle φ is relative to the shear deformation. During Vertical bearing capacity tests, the friction angle reaches a minimum value φ_{res}. However, during horizontal pushover tests with $FS_v > 1$, the friction angle of the soil is much larger, which consecutively leads to larger Safety factors than those calculated traditionally and thus larger bearing capacity..

Cyclic Loading

The same models we submitted to the aforementioned cyclic protocol TYPE I, consisting of 14 cycles of increasing amplitude. Results are shown in **Figure 3.4** Switching to cyclic loading, similar results can be observed. In terms of Moment-Rotation and comparing to the monotonic backbone curves, it can be said that the smaller the FS_v the larger the overstrength displayed. Actually, for the light foundation it is evident that the cyclic loops are enclosed in the monotonic curve. In addition to that, we can see that for small safety factors, the loops demonstrate an oval shape, whereas for the high safety factor the loops are clearly S-shaped. This S-shaped loop derives from the fact that for high factors of safety and large amplitudes of displacement, the soil underneath the foundation curves and the foundation loses contact with the soil. When the direction of the load changes, the foundation only partially

touches the ground, and has to close the gap formed, thus the reduced rotational stiffness.

In terms of settlement-Rotation, Shown in **Figure 3.5**, as was projected from the monotonic curves, the heavier the structure, the more settlement it accumulates per cycle and the less uplift is noticed for large amplitude cycles. This is reasonable as Low FS_v models tend to settle even for small amplitudes, something that is mainly attributed to the larger stresses transmitted because of the increased weight. The same results can be observed from **Figure 3.6**, showing the evolution of settlement with regard to the number of cycles and accumulated settlement for each amplitude of imposed displacement. It is evident that for larger amplitudes, the difference in settlement between the three different models increases. This happens because models with higher FS_v demonstrate more uplift than sinking in larger amplitudes comparing to models with low FS_v, whereas in small amplitudes all models demonstrate sinking varying only in absolute values.

3.2.2 Same mass-different soil-two cases

An effort was made to investigate the response of two systems with the same superstructure lying on different sand strata. To this end, the two foundations with dead load of 35kg and 100kg we tested on different sand types with D_r of 45% and 65% respectively, giving vertical safety factors of 5 and 2.6. **Figure 3.7, 3.8** and **3.9** displays the results for Monotonic and cyclic loading of the two aforementioned models, compared to their counterparts lying on dense sand. As far as monotonic loading is concerned, the results are similar to what we expected. In terms of Moment-Rotation, both systems demonstrate smaller Bearing capacity comparing to the ones founded on dense sand, which is attributed to the soil being of poorer quality. Also, in accordance with the FS_v being smaller, the two cases display smaller overturning angles as more soil yielding takes place.

Regarding the cyclic Loading, for the case of the 100kg superstructure model, there does not seem to be any striking difference between the two cases as the difference in FS_v is not very large. Contrary to that, for the case of the 35kg model, the near tripling of the FS_v changes the shape of the loops completely, as was seen on the previous chapter. It can also be observed that the overstrength factor is larger for smaller values of the FS_v. Actually in terms of maximum moment achieved, both models display almost the same value for cyclic loading in the two extreme cases.

A large difference can be noticed in the w-θ diagrams. More specifically, the lightweight structure that demonstrated an obvious uplift dominated

response when lying on dense sand, now shows a much more sinking dominated behavior, and the settlement is substantially larger. For the heavy model, although, for the cyclic tests, the qualitative change in the shape of the curve is not evident, the residual settlement is almost double. This is in agreement with the monotonic curves though, where the model lying on dense sand demonstrates some uplift for larger amplitude cycles.

3.3 The Effect of the Change in Load Protocol

To be able to further investigate the effect of multiple cycles, several load protocols of imposed displacement were imposed. **Figure 3.10** displays a comparison of the three different Loading protocols in terms of Moment – Rotation and Settlement - Rotation.

The M-θ charts evidently show that the shape of the loops for all three load types is similar. Rotational stiffness does not seem to be affected by the number of cycles or by previous loading steps. Apart from that, the overstrength factor compared to the monotonic curve, for the same amplitude of imposed displacement is also similar for all the systems.

In Terms of w-θ, as expected, load type III displays the most residual settlement, followed by Load Type I and Load Type II. This is attributed primarily to the larger number of cycle imposed. Again, it is interesting to notice that for small amplitudes and the same range of imposed displacement,

the settlement accumulated is very similar for all Load types. Comparing to the monotonic curve, the three models display similar behavior with sinking dominated response for small and medium rotating angles and a tendency to uplift for larger angles. In effect, sinking or uplift is only dictated by the range of the imposed rotation and not by the previous load history. **Figure 3.11** shows, in overview, the evolution of settlement for the three different Load Protocols. As expected, Load Type II displays the least settlement, followed by Load Type I and Load Type III. This difference should be attributed purely to the number of cycles imposed in each Load Protocol. Generally, more cycles lead to more settlement and so on.

3.4 The Effect of Soil Density D_r

At this point, it would be worth making a comparison between two systems with the same factor of safety against vertical load but lying on different soil. The FS_v is regarded as a strong equivalency factor between two systems, so knowing the differences between the two could help understand which sizes are comparable. The two models compared are the 100kg superstructure lying on the dense sand stratum, and the 35kg superstructure lying on loose sand. **Figure 3.12** displays the results in Terms of Moment-rotation and the evolution of settlement. In terms of M-θ, although no direct comparison is viable, there is a clear difference in the overstrength factor developed during cyclic loading, in relation to their respective monotonic

curves. The one on loose soil clearly demonstrates a much bigger overstrength factor. Apparently, due to soil densification, the quality of the soil improves, giving this larger overstrength.

In terms of settlement, it can be said that the model lying on loose sand demonstrates larger values. This can be attributed to the fact that loose sand tends to densify, thus further reducing its void ratio and increasing settlement, whereas dense sand tends to loosen, developing a contrary behavior. Another interesting remark can be made when comparing the settlement accumulated per cycle for Load protocols I and III on the two models. It is clear that the relative increase of settlement from one type of loading to another is larger for the model lying on the dense sand, for the same reasons explained above. In fact, in the end, the two models have accumulated the same settlement, with the model on loose sand showing a steady evolution and the one lying on loose sand having a rapid increase for cycles of larger amplitude.

3.5 Comparison - Validation to past Tests (PWRI)

In order to receive some validation from the scores extracted throughout this series of tests, the results were compared to large scale 1g experiments realized at the Public Works Research Institute, Tsukuba, Japan. In the effort to compare similar models, cases 10 and 11 from the cyclic tests were chosen

for comparison. **Figure 3.13** displays a draft view of the two scenarios compared. These consist of a square footing lying on dense sand with a slenderness ratio (H/B) of 1.8 a Safety factor against vertical Loading of 16, subjected to two different loading protocols similar to Load Type I and Load Type III that have been used in this series. **Figure 3.14** displays a comparison between case 10 and one of the aforementioned tests with Dense Sand and FS_v = 14 subjected to cyclic Loading Type I and case 11 to the same model subjected to cyclic Loading Type III. Taking into account the reduced scale of our series of tests and adding to that the fact that the slenderness ratio is not very similar, something that in our case would account for more rocking and less sliding dominated behavior, the comparison points out that the two series display, qualitatively, similar results. This serves as an encouragement that the results of this series can be adequately taken into consideration.

FIGURES

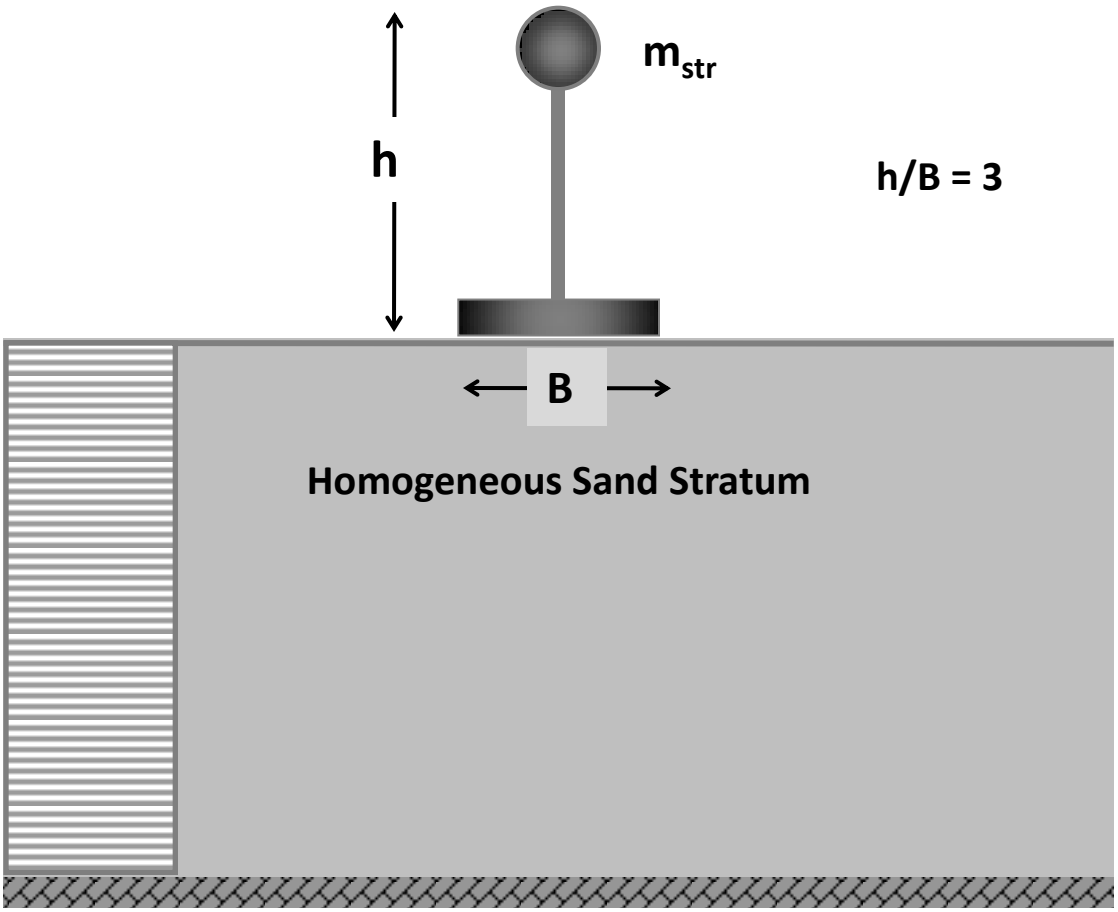

Figure 3.1. Draft view of the Model investigated in the experiments

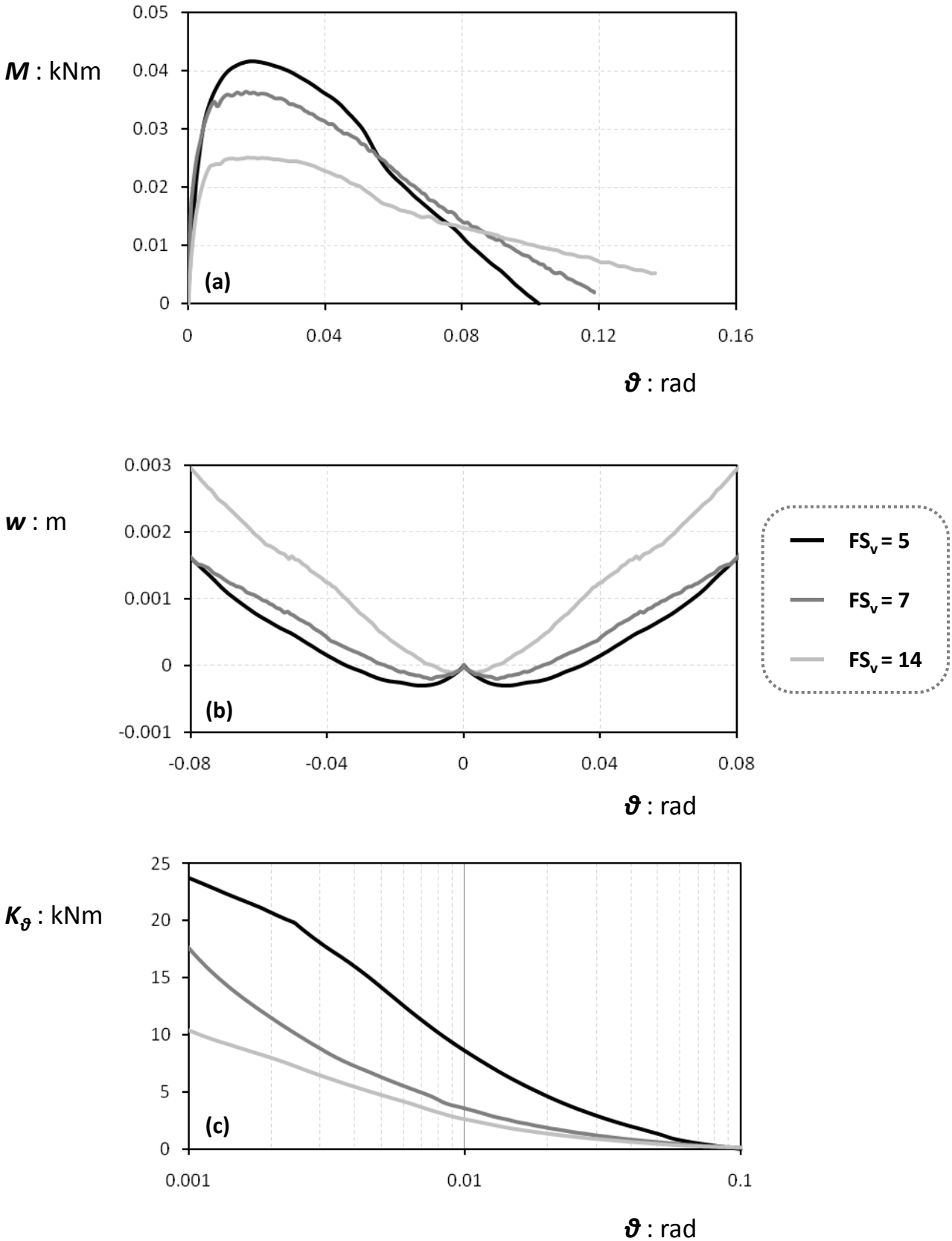

Figure 3.2. (a) Moment–rotation curves, **(b)** settlement–rotation curves, **(c)** rotational stiffness curves derived from monotonic pushover tests for systems with FS_v = 5, 7 and 14 (lying on dense sand D_r = 93 %).

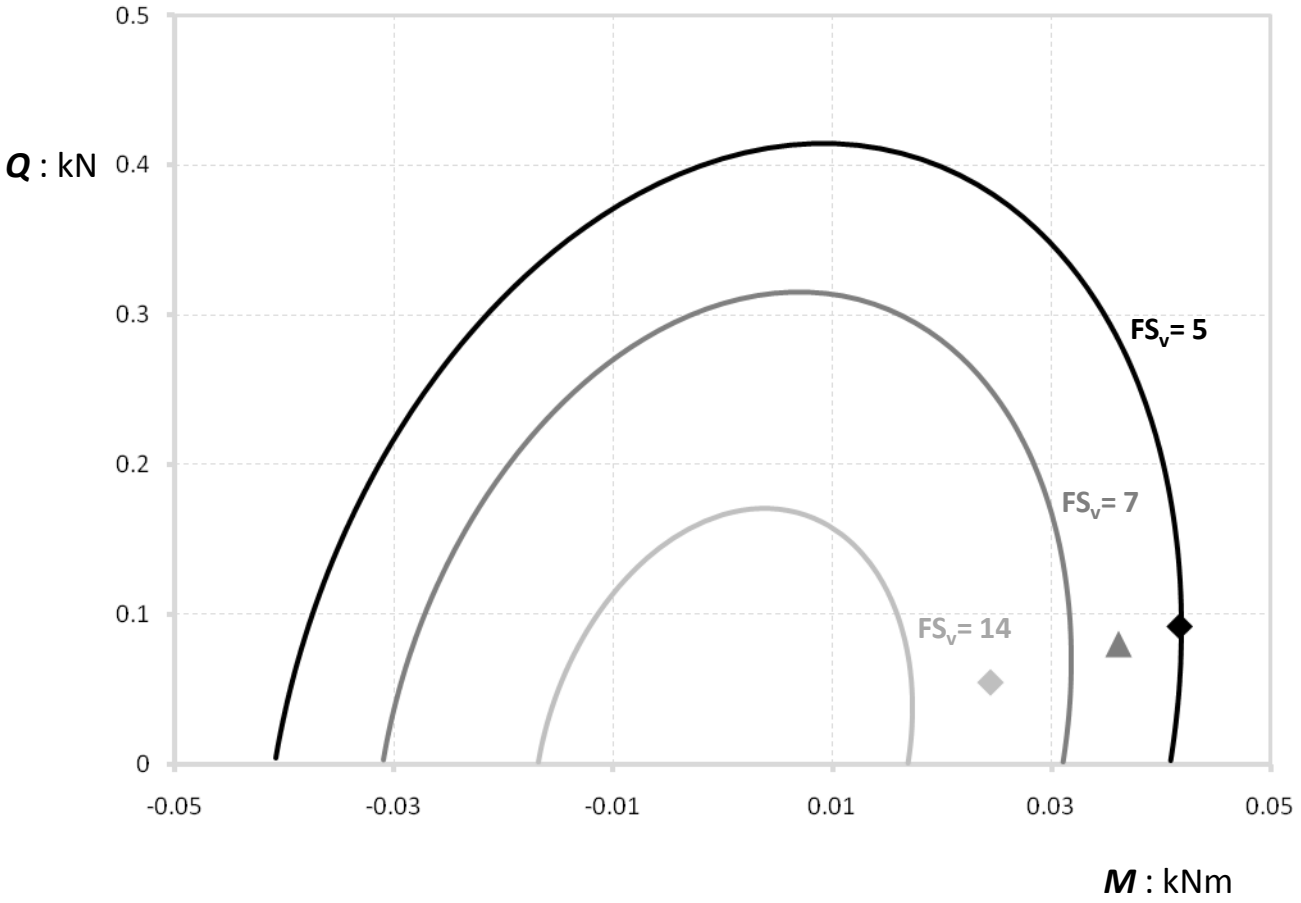

Figure 3.3. Comparison in the *Q : M loading plane* between the failure envelopes derived by Butterfield & Gottardi (1994) and the experimental results for FS_v = 5, 7 and 14.

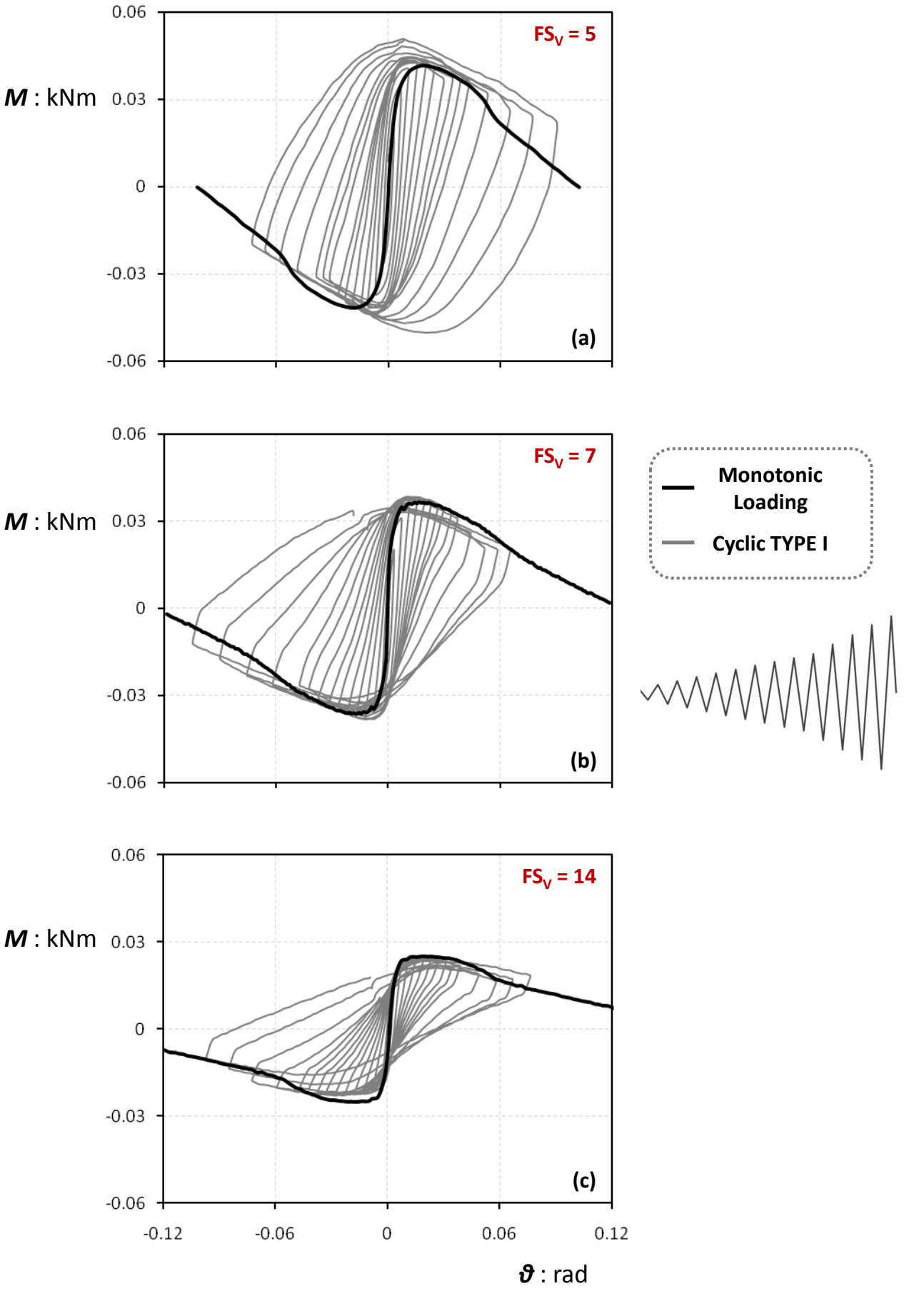

Figure 3.4. Moment–rotation curves derived from slow cyclic pushover tests (**TYPE I**) for systems with FS_V **(a)** 5**, (b)** 7 and **(c)** 14 (lying on dense sand D_r = 93 %). The black lines correspond to the monotonic backbone curves.

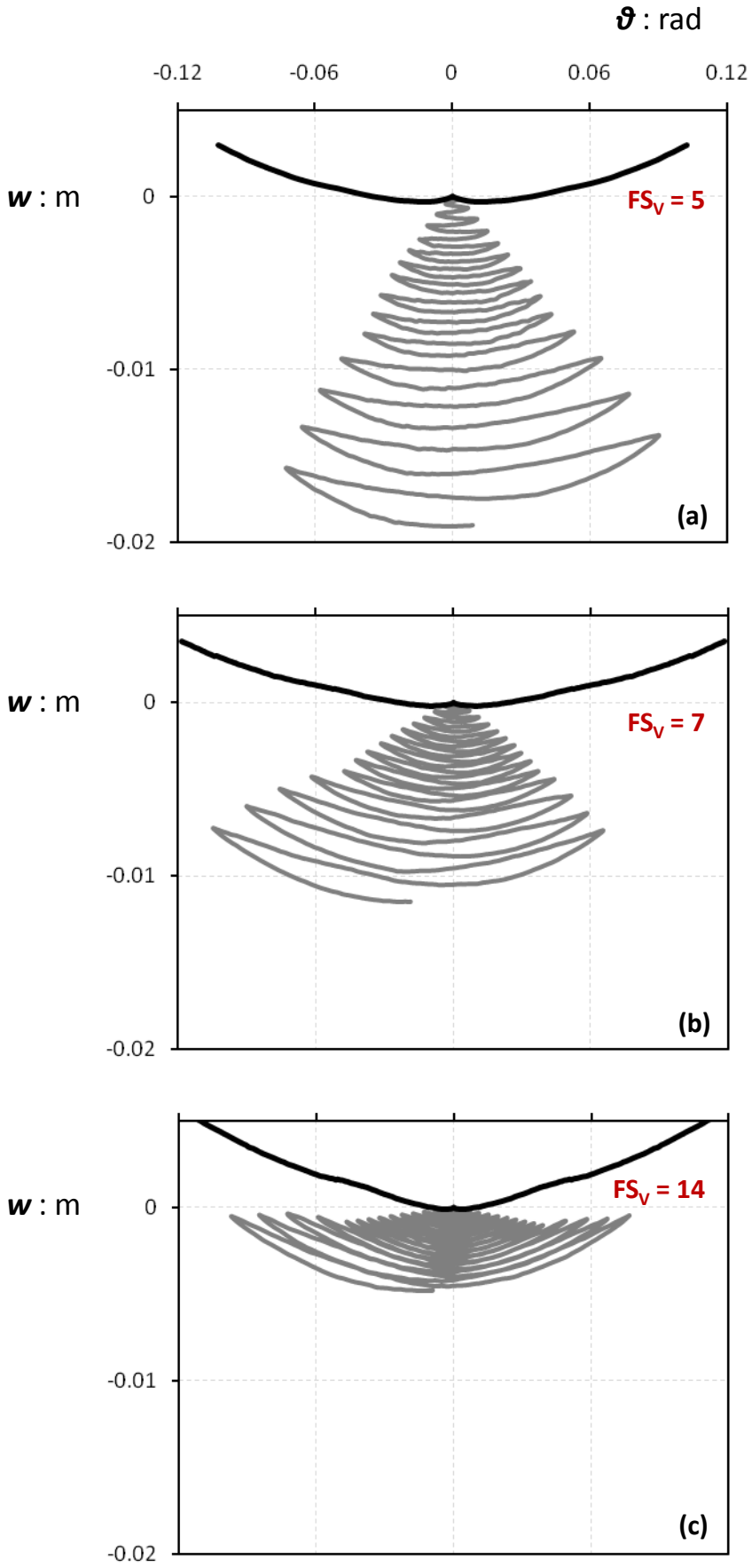

Figure 3.5. Settlement–rotation curves derived from slow cyclic pushover tests (**TYPE I**) for systems with FS_V **(a)** 5**, (b)** 7 and **(c)** 14 (lying on dense sand D_r = 93 %). The black lines correspond to the monotonic backbone curves.

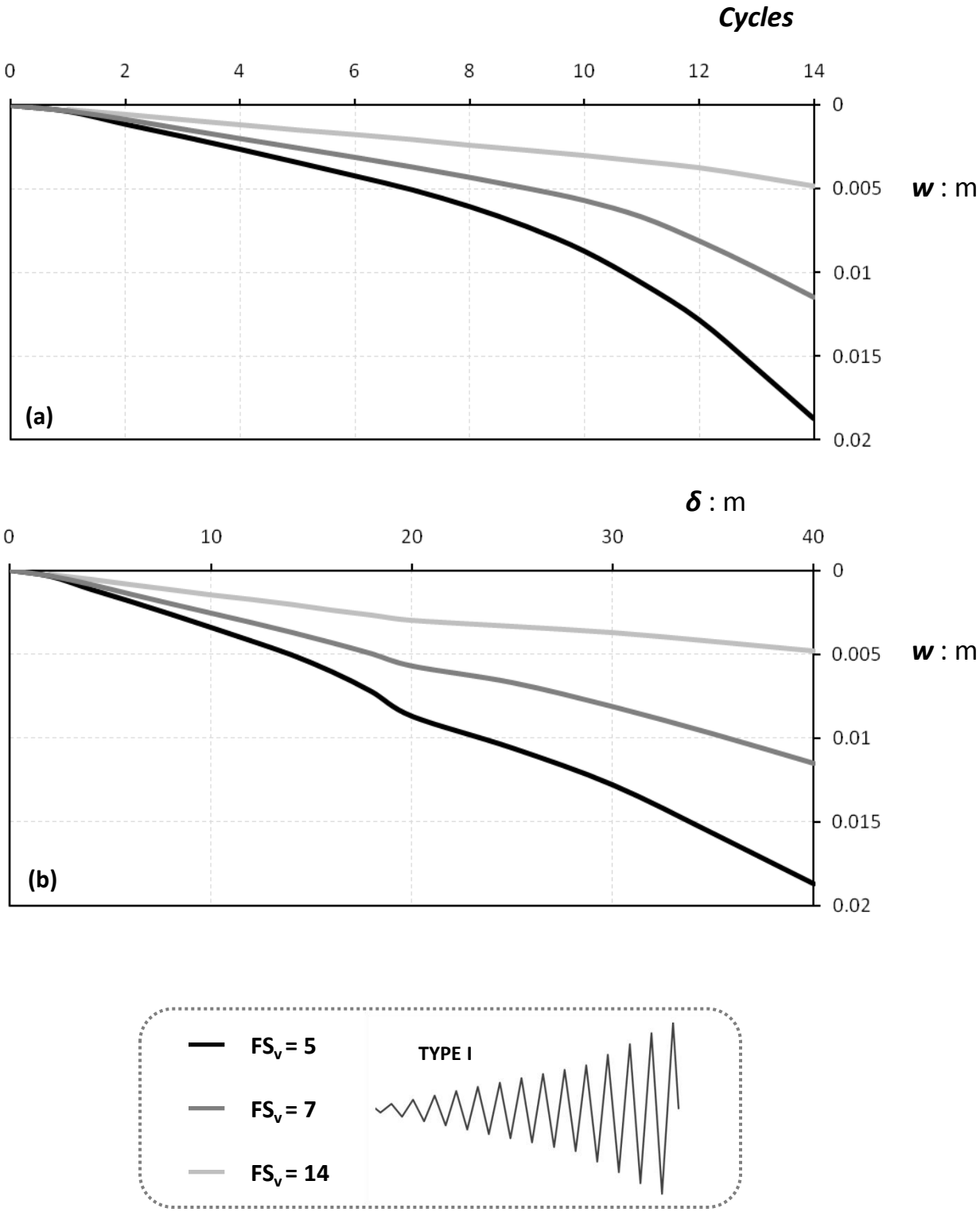

Figure 3.6. (a) Settlement per cycle and **(b)** settlement per imposed horizontal displacement derived from slow cyclic pushover tests (**TYPE I**) for systems with FS_v = 5, 7 and 14 (lying on dense sand D_r = 93 %).

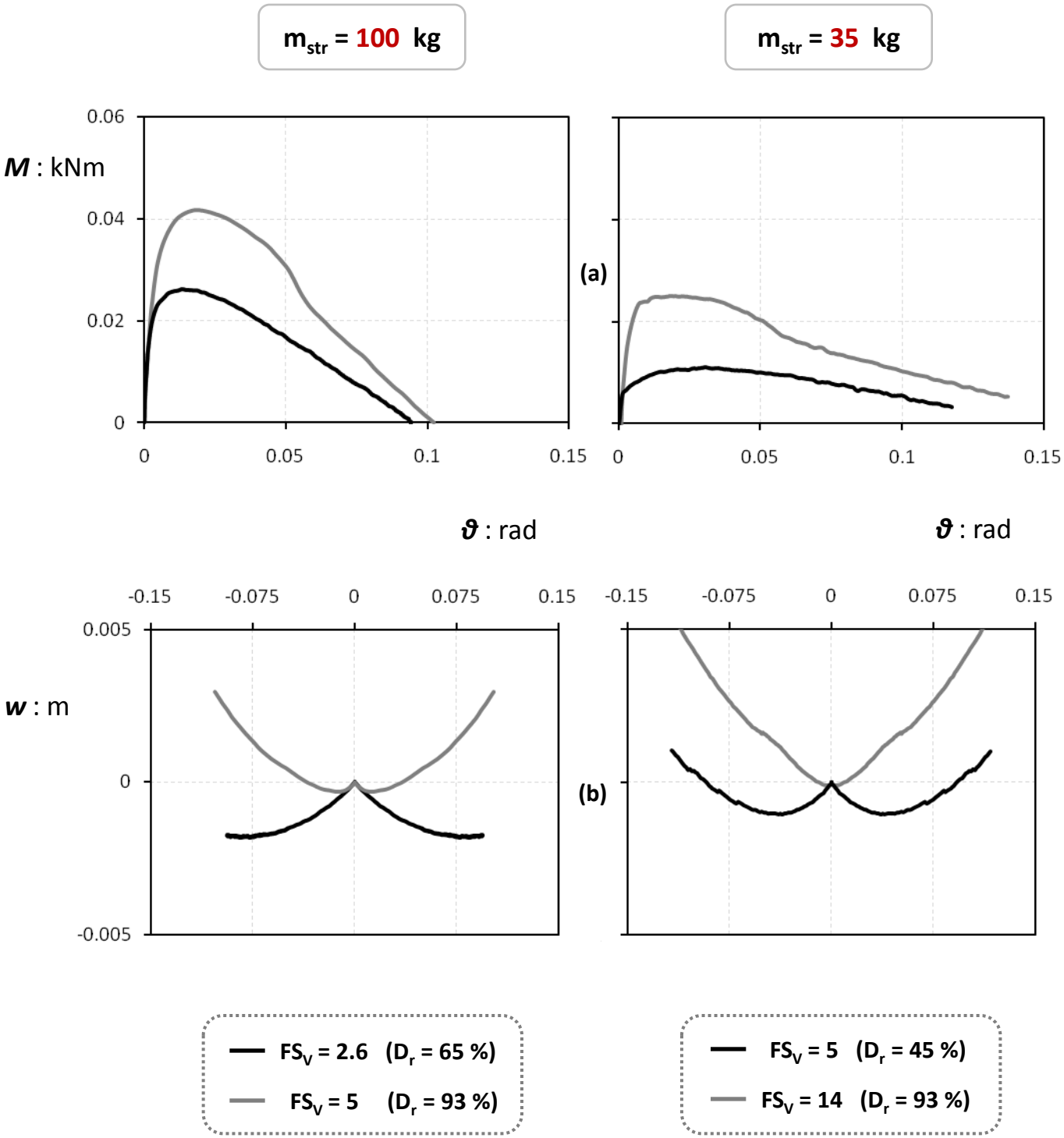

Figure 3.7. (a) Moment–rotation and **(b) s**ettlement–rotation curves derived from monotonic pushover tests for systems with different factors of safety, lying on strata of varying relative density.

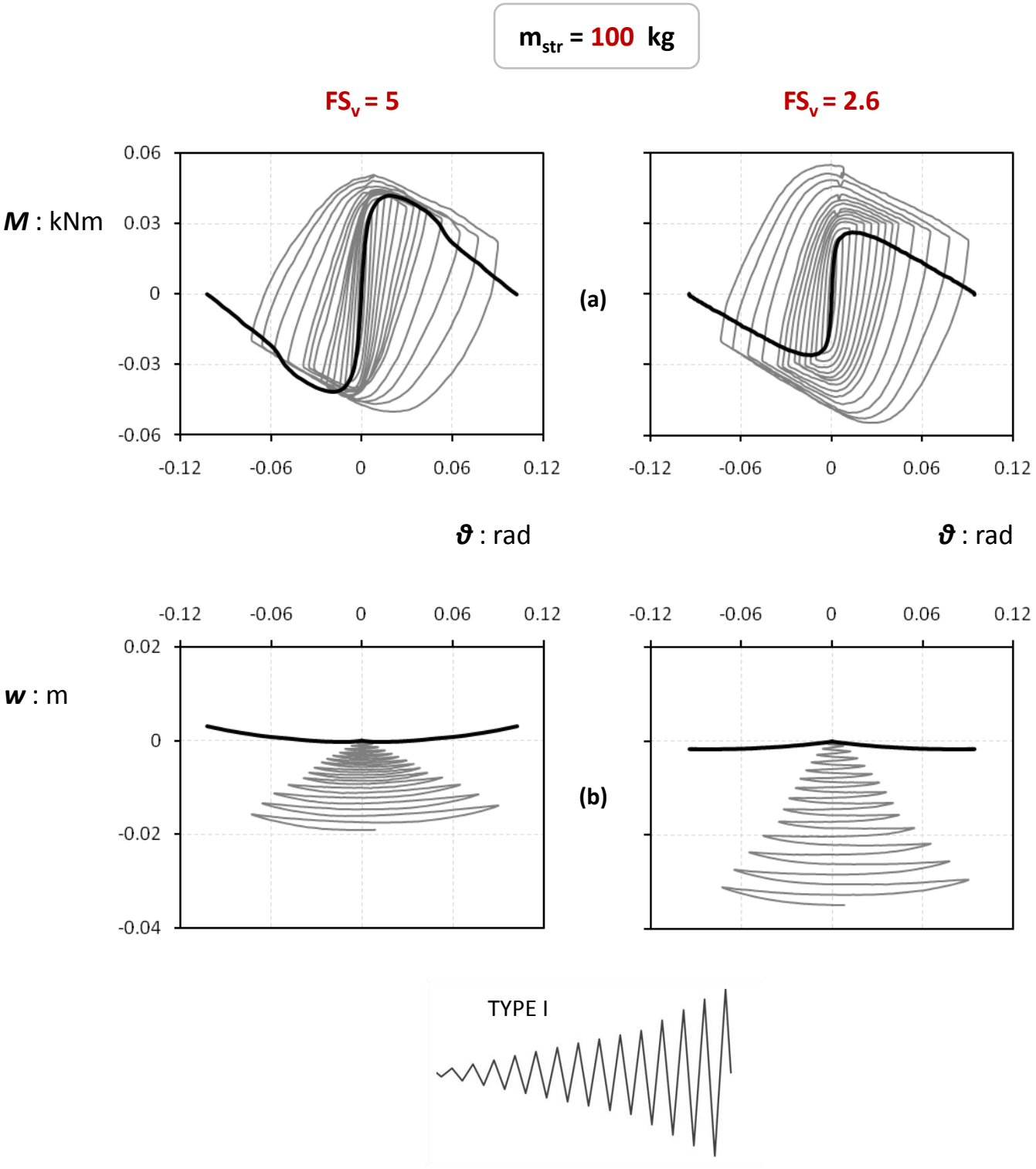

Figure 3.8. (a) Moment–rotation and **(b)** settlement–rotation curves derived from slow cyclic pushover tests (**TYPE I**) for systems with structural mass $\mathbf{m_{str}}$ **= 100 kg** lying on sand of relative density D_r = 93 % (**FS_V = 5**) and D_r = 65 % (**FS_V = 2.6**).

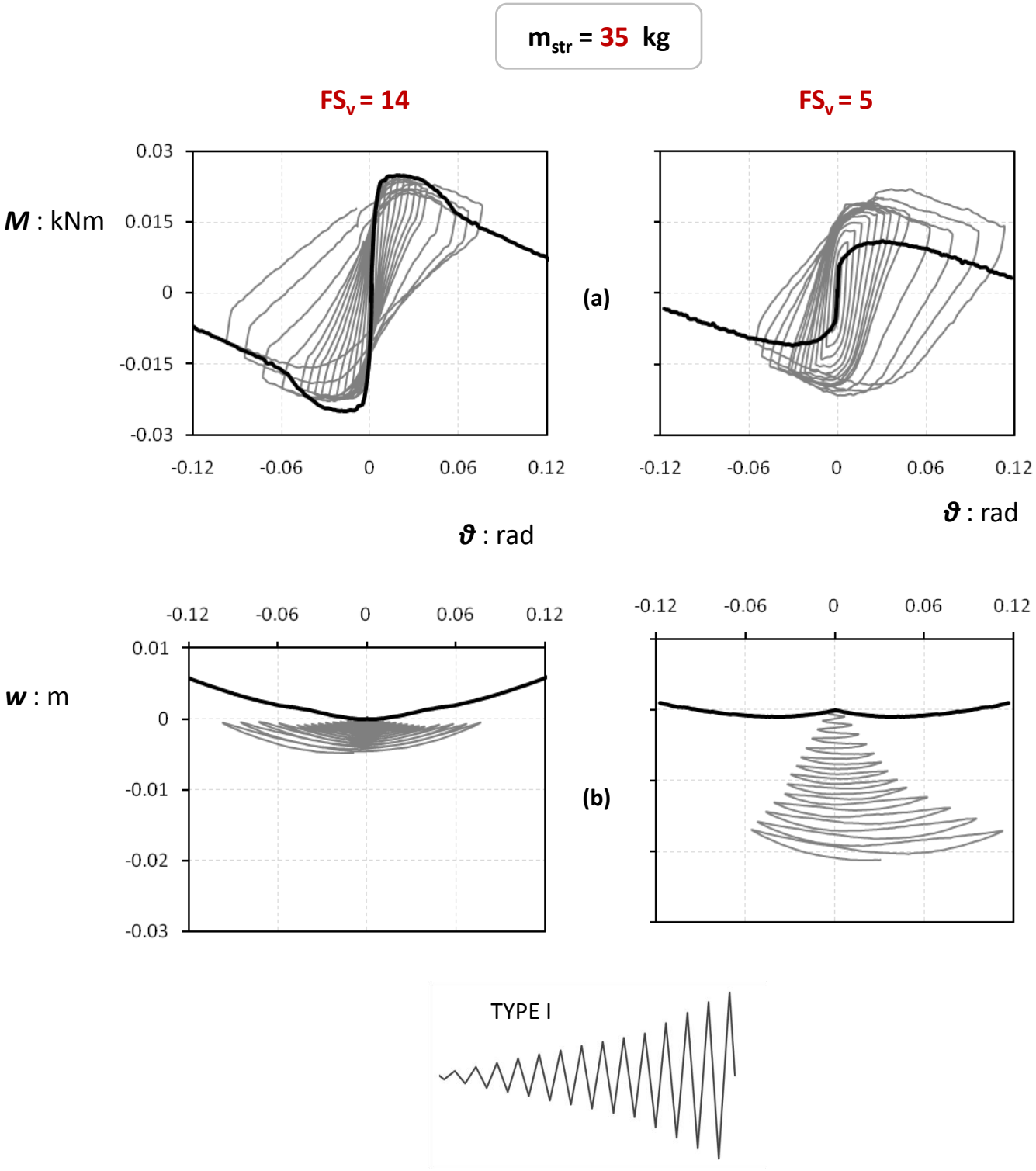

Figure 3.9. (a) Moment–rotation and **(b)** settlement–rotation curves derived from slow cyclic pushover tests (**TYPE I**) for systems with structural mass $\mathbf{m_{str}}$ **= 35 kg** lying on sand of relative density D_r = 93 % (**FS_V =14**) and D_r = 45 % (**FS_V = 5**).

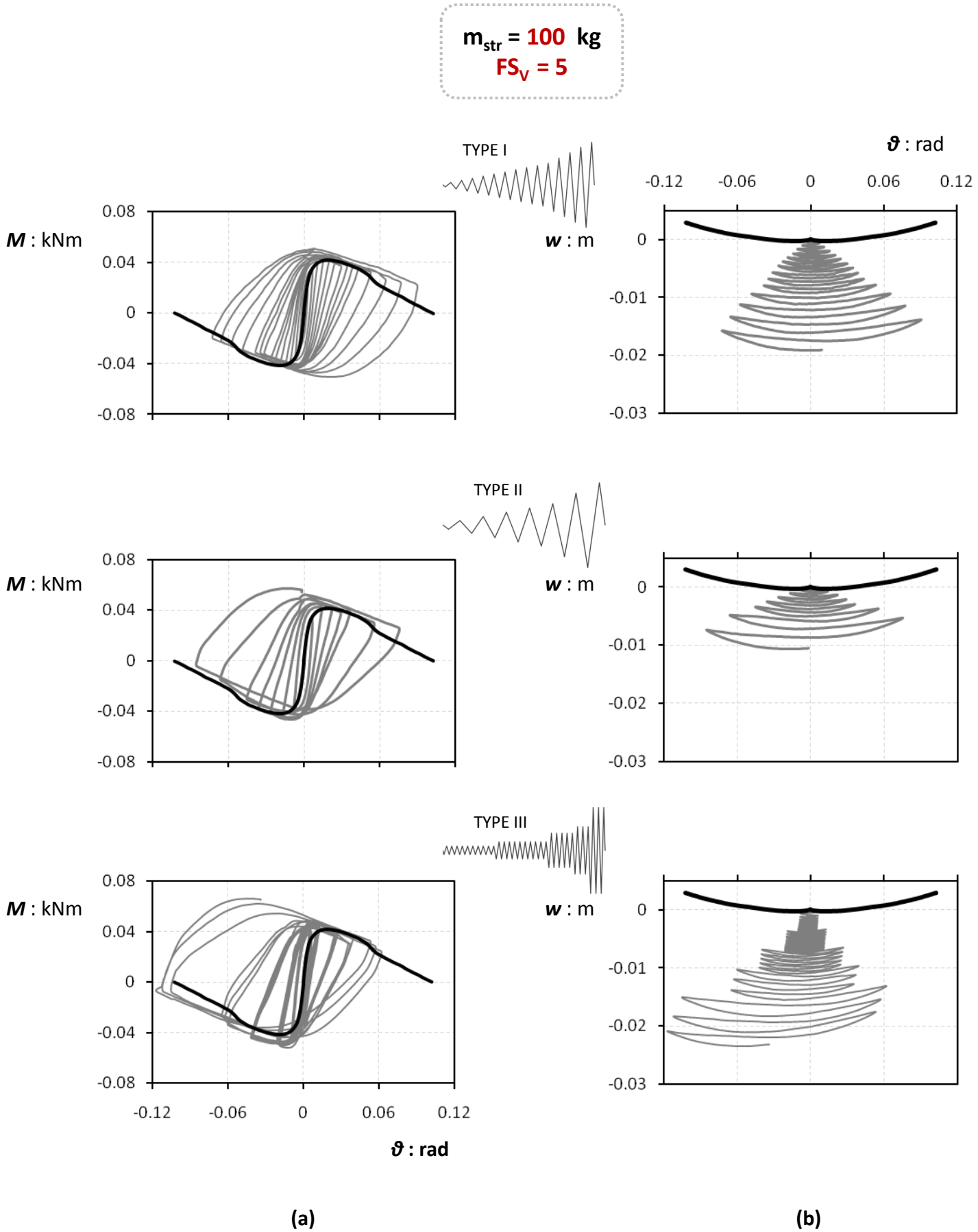

Figure 3.10. (a) Moment–rotation and **(b)** settlement–rotation curves derived from slow cyclic pushover tests of different loading protocols. The structural mass is $\mathbf{m_{str}}$ **= 100 kg** and the sand relative density $\mathbf{D_r}$ **= 93 %**.

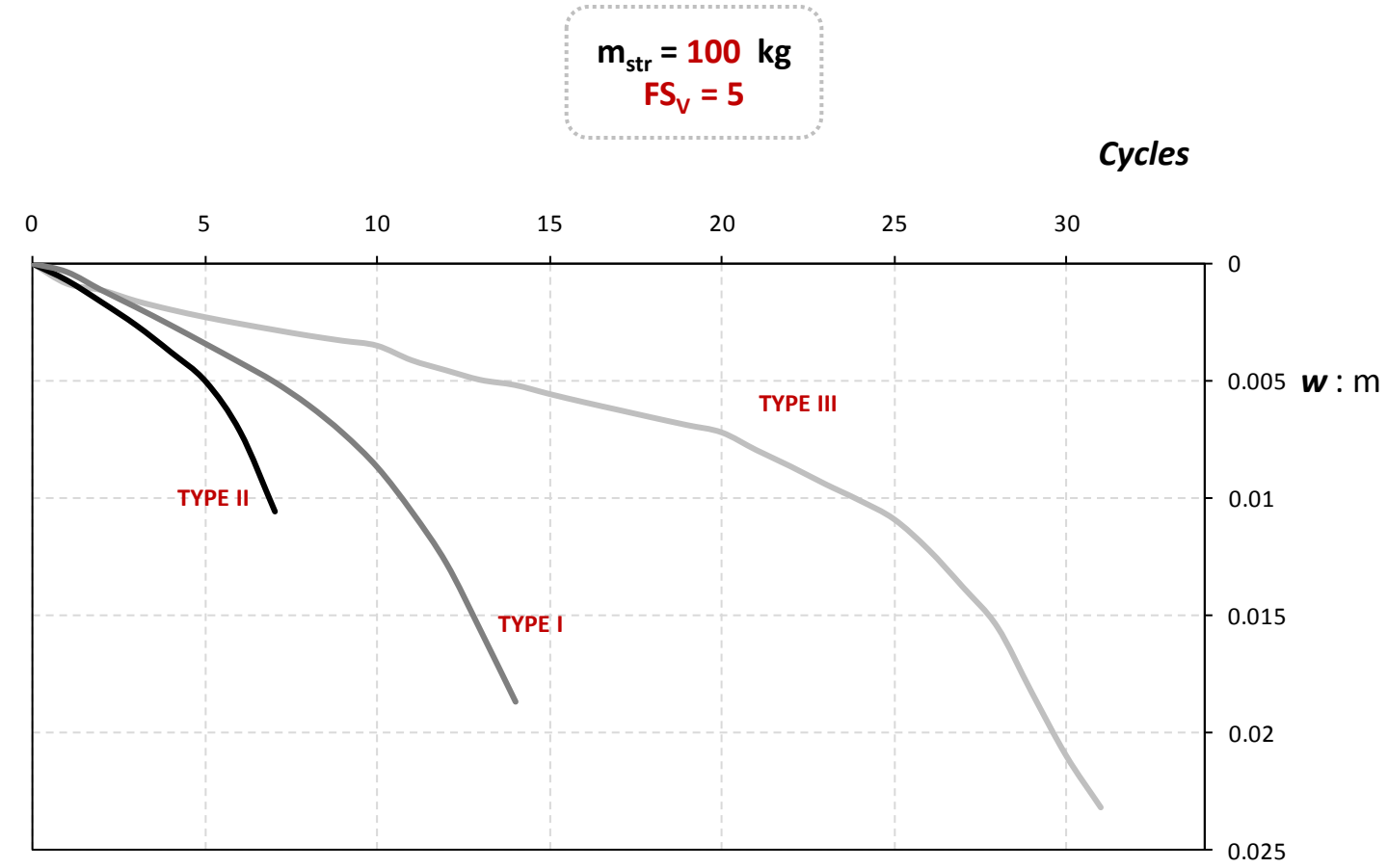

Figure 3.11. Accumulation of settlement with respect to the number of cycles during slow cyclic pushover loading of different types. The structural mass is $\mathbf{m_{str}}$ **= 100 kg** and the sand relative density $\mathbf{D_r}$ **= 93 %**.

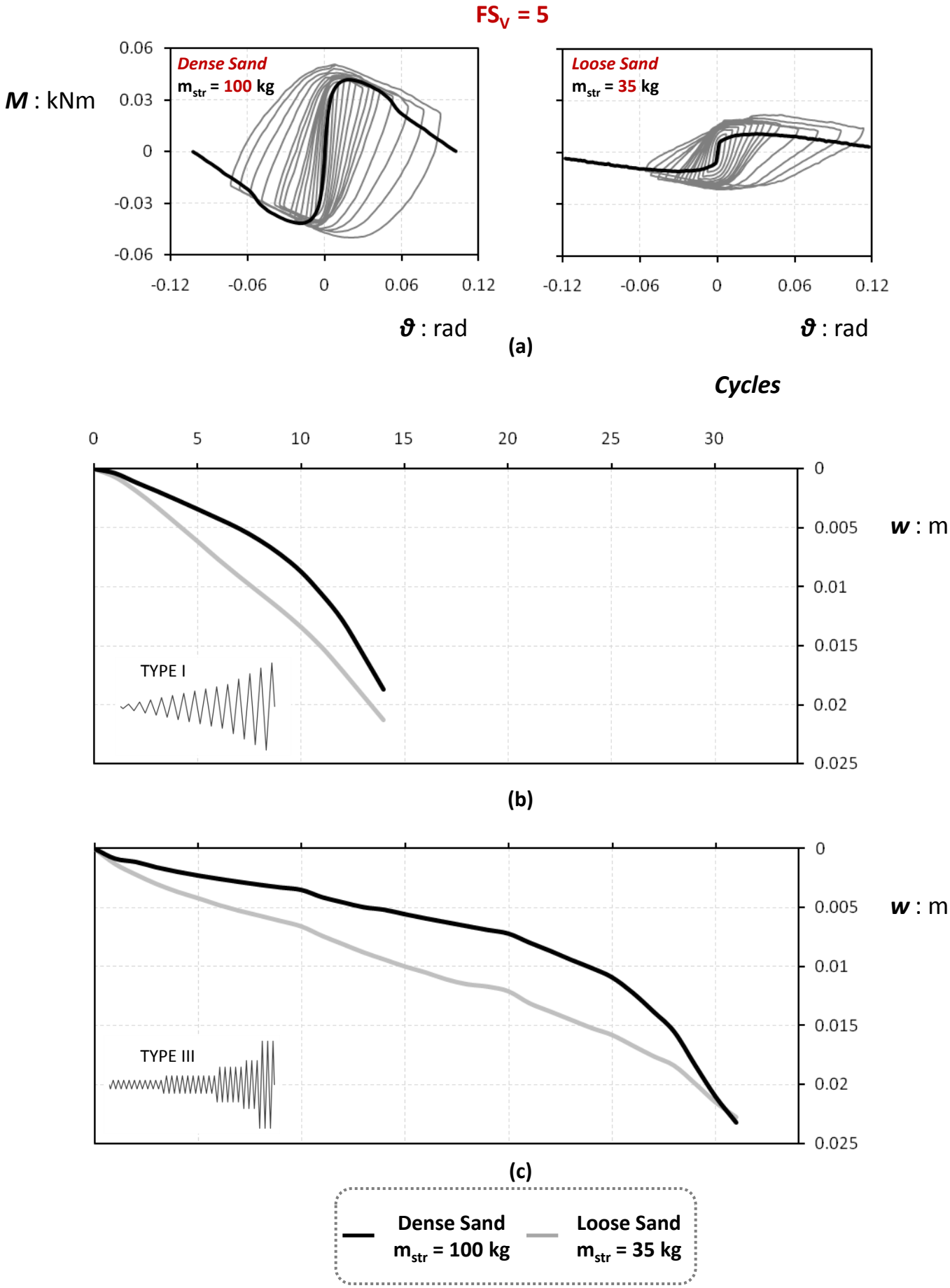

Figure 3.12: (a) Moment–rotation curves and accumulation of settlement with respect to the number of cycles during slow cyclic pushover tests **(b)** TYPE I and **(c)** TYPE III. The compared systems have the same FS_V= 5, lying on sand of different relative density.

NTUA : *Reduced scale 1g experiment*

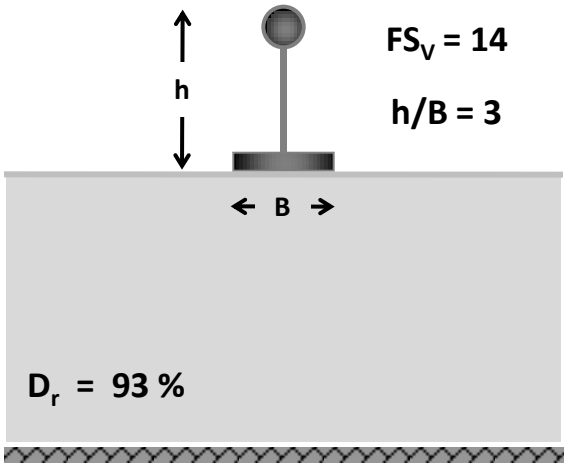

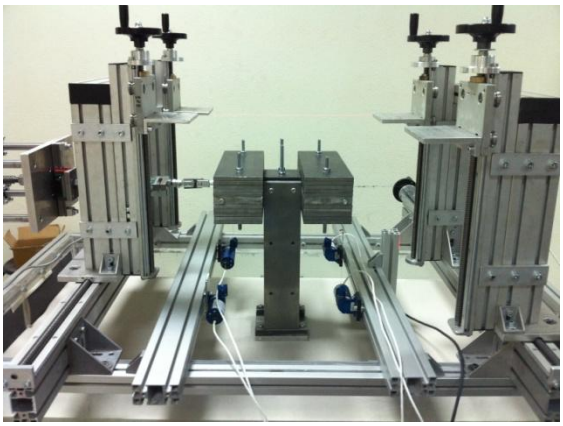

(a)

PWRI : *Large scale 1g experiment*

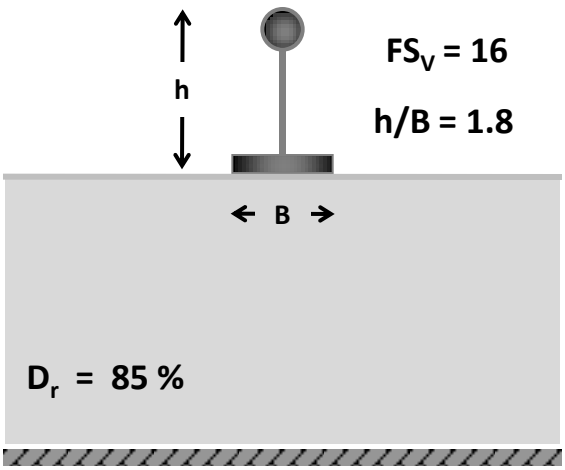

(b)

Figure 3.13. Schematic illustration and picture of **(a)** the system investigated herein and **(b)** the system examined at PWRI (photograph from Paolucci et al, 2008).

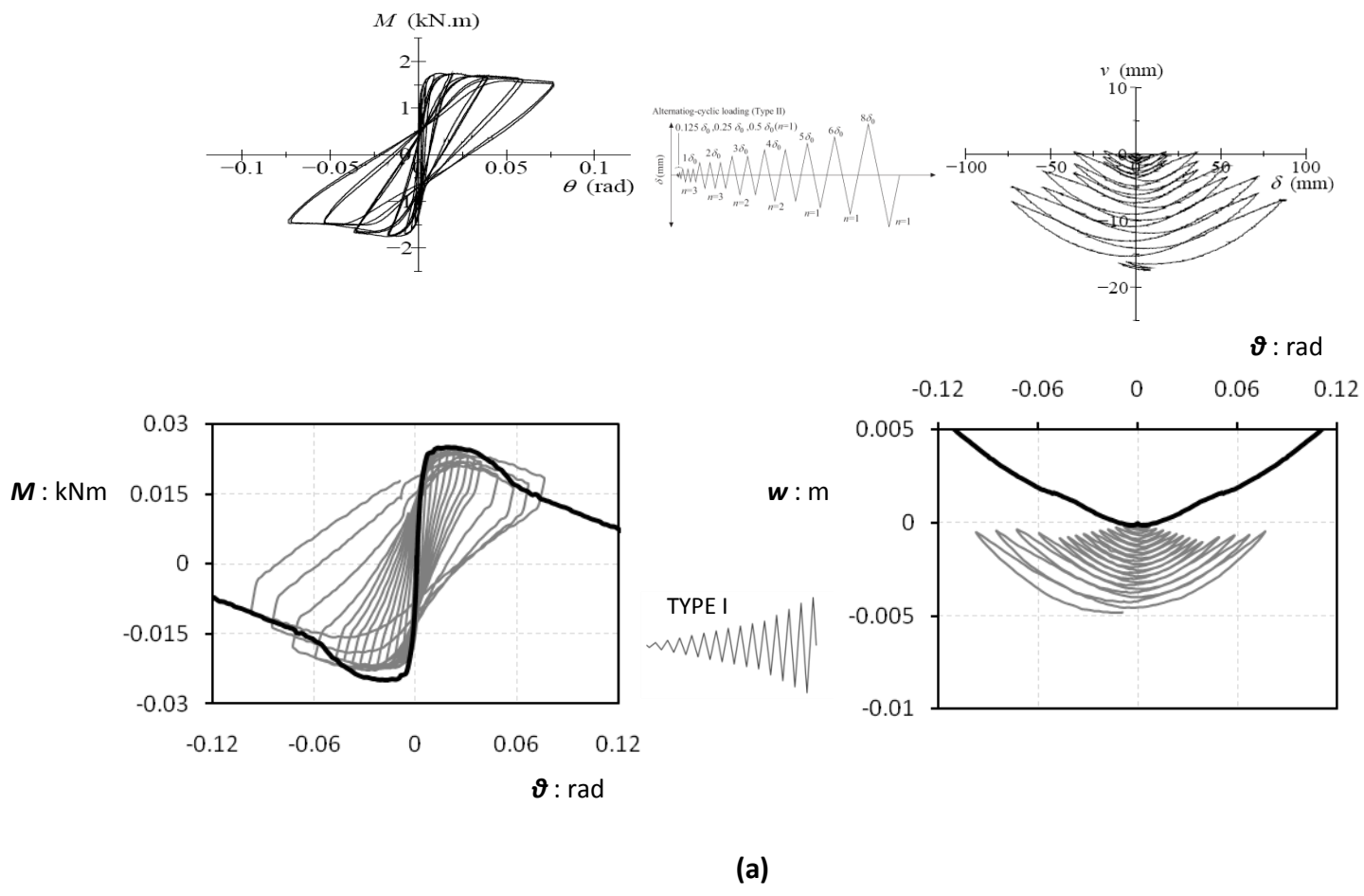

(a)

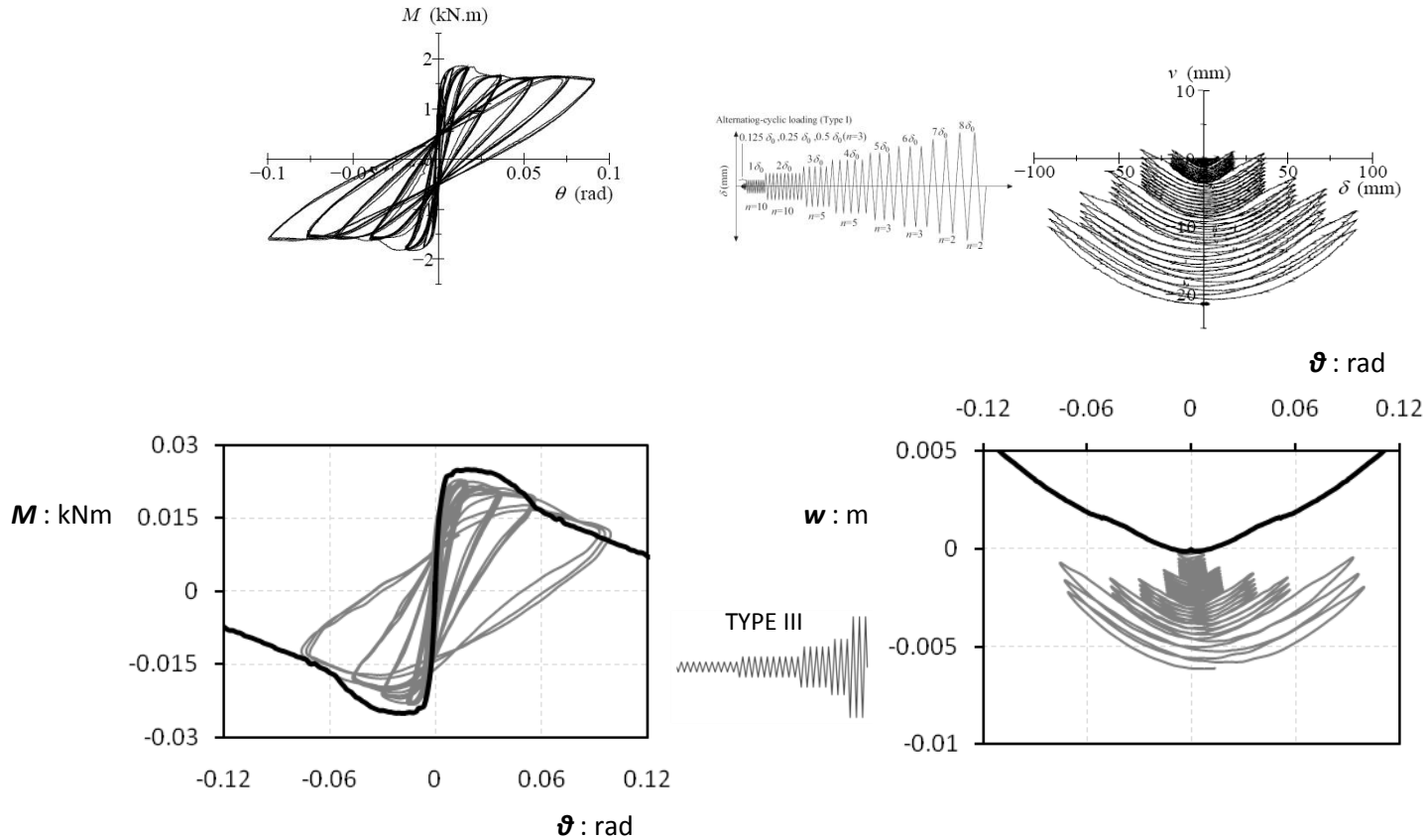

(b)

Figure 3.14. Qualitative comparison between the experiments conducted at **PWRI** and **NTUA** in terms of moment–rotation and settlement–displacement (rotation) curves for **(a)** one cycle per horizontal displacement amplitude and (b) many cycles per horizontal displacement amplitude.

Chapter IV:

Shallow Soil improvement : 35kg Foundation Investigation

4.1 Introduction

Achieving a satisfying rocking behavior from the superstructure-foundation-soil system obviously has its benefits as imprinted in the introduction and illustrated in the previous chapters. However, as it was also shown, the price to pay comes in terms of residual settlement, especially for low vertical factors of safety, where behavior is dominated by sinking.

Driven by this thought and by the fact that rocking mechanism does not have a deep area of effect, we can try to achieve the desired foundation response by improving the soil at a very shallow depth. This “shallow soil improvement” could give us the added benefits of superior soil quality for the small price of adding an “extra” layer of soil.

To evaluate the effectiveness of this idea, two systems were investigated. The first consist of the “lightweight” structure (35kg mass) lying on loose sand, with the improvement ranging between a quarter and a full breadth of the foundation in depth, made of Dense Sand. The concept behind this choice was to see the effects of soil improvement on a structure for which the two extreme

cases displayed a totally different behavior, from sinking dominated to almost completely uplifting dominated, with minimal settlement.

The second system consists of the “heavy” structure (100kg mass) lying on sand of medium density, with the improvement of dense sand ranging from half to a full foundation breath. Although, as previously discussed, contrary to the first system, the behavior between the two extreme cases was not very different qualitatively, this investigation was primarily aimed at how the shallow soil improvement can help reduce residual settlement after strong earthquake shaking, which is the largest price to pay for allowing foundation rocking.

4.2 35kg Foundation

Monotonic loading

Figure 4.1 displays the three different cases of soil improvement investigated, along with the two extremes of homogeneous sand stratum. To be able to analyze the results, the models were first subjected to Horizontal monotonic loading. The results from the tests are displayed in **Figure 4.2**. In

terms of Moment- rotation, it is obvious that the Maximum moment achieved rises with the increase in the depth of the soil improvement. This is reasonable, mainly due to the fact that the overall soil quality increases with the increase in the depth of the soil improvement. Unfortunately, it was not possible to continue all the tests up to the overturning angle. However, it could be concluded from the shape of the curves that the overturning angle also increases as the depth of the soil improvement increases. This is also something to be expected, as the increase in soil improvement reduces the extent of soil plastification and soil deformation, and the model approaches the behavior of rocking on a rigid base.

Comparing the results in terms of settlement-rotation, it can be seen that with an increase in the depth of soil improvement, the foundation tends to uplift more and for a much larger range of rotation. As the foundation uplifts, the effective foundation breadth in contact with the soil reduces. Because of that, the size of the stress bulb, which is relative to the effective breadth, reduces. In effect, the stresses reach shallower depth, and the effect of the improved soil's stiffness increases. Effectively, the foundation responds as if founded on a stiffer soil, so the uplift increases. There seems to be some inaccordance for cases of dense sand and the one with soil improvement of z/B=1. For larger amplitudes of loading, the latter one displays more uplift, which is not reasonable. This could possibly be attributed to some kind of flaw in the experimental setup for the former test, as the curvature of the line changes unexpectedly after some point. However, judging from the rest of the

chart, it would be fair to say that there is no obvious difference between the two curves, as well as between the curves of the foundation lying on loose sand and the one lying on soil improvement with z/B= 0.25.

The last chart compares rotational stiffness with respect to the amplitude of rotation. For a given superstructural mass, which governs the confinement stresses in the soil, as mentioned before, rotational stiffness should be relative to the Shear Modulus G, which is affected by sand density. This translates to larger stiffness for greater depths of soil improvement. This is visible in the chart, except for very small rotations, where the loose sand displays more stiffness than the two models with soil improvement. This, however should not be regarded highly as there is generally some degree of difficulty in capturing the displacements for very small amplitudes. Disregarding that, it can be said that the model with the very shallow soil improvement doe not display any difference from the one lying on loose sand, and that the rest of the case show a proportionally increasing rotational stiffness.

Cyclic Loading

Moving from monotonic to slow cyclic loading, the results in terms of moment-rotation are displayed in **Figure 4.3** for loading protocol type I, along with the monotonic backbone curves. First, the two cases for homogenous soil, discussed in previous chapters, are shown. By comparing the results from the three models with soil improvement to the homogenous ones, it can be seen

that as the depth of soil improvement increases, the loops change from oval-shaped, resembling the Loose sand model, to S-shaped, similar to the ones in the dense sand model. Another interesting notice is that contrary to monotonic loading, all systems seem to display the same Moment capacity in cyclic Loading. In effect, this means that the overstrength factor decreases as the FS_v increases, similar to the models on homogenous soil discussed in the previous chapter.

In terms of settlement-rotation, **Figure 4.4** displays a comparison for the same type of loading. These charts show the change in behavior with respect to the depth of soil improvement. For the "shallower" improvement, the results are similar to the model lying on loose sand, except for a significant decrease in settlement. However the response is again strictly sinking dominated, thus the large settlement compared to the other two cases. The model with an improvement of z/B=0.5 displays an "in-between" behavior, with even smaller settlement and more uplift. Finally, for the model with the "deepest" improvement, the behavior is very close to the model lying on dense homogenous sand, both in terms of residual displacement and tendency to uplift. All these seem to be in accordance with the results from the monotonic curves.

Figure 4.5 displays a comparison for the same tests in terms of settlement per cycle and secant rotational stiffness per cycle with respect to the half-amplitude of the cycle. For the first chart, which displays the evolution of

settlement, it is evident that as the soil improvement increases in depth, the soil effectively mobilized becomes stiffer and of greater strength, so the settlement accumulated is reduced. More noticeable changes are noticed for leaping from the loose sand model to the one with an improvement of z/B=0.25 and from the latter to the one with z/B=0.5. For the model with z/B=1, the residual settlement is very close to the one of the model lying on homogeneous dense sand. Thus said, further increasing the depth of soil improvement would not seem to have a considerable effect in terms of residual settlement. Finally, the five models show much more similar values of displacement for small amplitude cycles than for larger ones. This can be attributed to the fact that for small cycles, there seems to be no or relatively small uplift. Due to that, the contact area between soil and foundation is larger and the stresses extend to a much larger depth. In effect, the quality of the improved soil does not play such a critical role because the poor soil below sustains a lot of the stress and accumulates the most settlement.

An effort was made to compute the degradation of secant rotational stiffness, with respect to the amplitude of displacement, meaning the half-amplitude of rotation imposed. The second chart shows an illustration of the way this was realized. The points of maximum rotation for each full cycle are chosen and the tangent of the angle of the line connecting them is the secant stiffness per cycle. For the five cases investigated, it is clear that the deeper the soil improvement, the larger the initial rotational stiffness with the two extreme cases being the model on loose sand, which has no improvement, and the one

on dense sand, where the "improvement" theoretically covers all the soil stratum. However, as the amplitude of the cycles increase, the rotational stiffness degrades to the point where all systems have similar values.

Load protocol comparison

As aforementioned, the amplitude of a cycle plays a vital role to the behavior of the foundation. Real earthquakes generally demonstrate a large variety of amplitudes and number of cycles. To be able to better evaluate the performance of shallow soil improvement in real earthquake loading, all models were subjected to cyclic loading protocol type III. This protocol displays a smaller variety of displacements, but also more cycles at smaller and larger amplitudes, giving the opportunity to better estimate the effectiveness of our systems for all kinds of loadings.

Figure 4.6 compares the results for the two loading protocols and the three different depths of soil improvement in terms of moment-rotation. Comparing maximum Moment achieved, both loading types demonstrate the same values, meaning that maximum moment achieved for each cycle is only relative to the amplitude of the cycle and not to the loading prehistory. Also, for Type III loading, there seems to be no degradation in rotational stiffness for the same amplitude of cycles, as discussed in previous chapters. Finally, comparing the shape of the loops for the two loading types, they seem to display the similar shapes for same depths of soil improvement.

In terms of settlement-rotation, **Figure 4.7** the comparison between the different loading types shows varying results for the three depths of soil improvement. For z/B=0.25 Type III loading clearly displays increased settlement comparing to Type I. On the opposite end, z/B=0.5 displays a smaller settlement for Type III loading and finally, z/B=1 has practically the same residual settlement for all load types. Due to the fact that the two load types display different number of cycles at different amplitudes of displacement, it is not easy to extract a direct relation between accumulated settlement and Load Type. The difference between the three models can be mainly attributed to the fact that that they demonstrate different behavior for different amplitudes of rotation, as indicated by the monotonic loading curves. So since the amplitude content of the two load protocols in not exactly the same, a model may display more settlement for the Type I protocol, even thought it includes fewer cycles, because the cycles are realized in a given amplitude where, according to the monotonic curve, the response is sinking dominated.

The evolution of settlement is shown in **Figure 4.8**, for both Load protocols. In load Type I the five models seem to display a proportional decrease in settlement with increasing depth of soil improvement. The difference in accumulated settlement is generally proportional to number of cycles already imposed and is not specifically associated to a certain amplitude. On the other hand, in Load Type III, where multiple cycles are imposed in a given amplitude, two trends seem to develop. The loose sand and the z/B=0.25

models display similarly large residual settlement, while the settlement in other three models is noticeably smaller. It is easily noticed that the larger proportion of the settlement for the z/B=0.25 model and one lying on loose sand is accumulated during small and medium amplitude cycles. For the other three models, the settlement accumulation is, as in Load Type I, more gradual. It can be seen that whatever difference is displayed between the two loading types can be attributed to the large number of small amplitude cycles where all models and especially the ones with small depth or no soil improvement at all demonstrate strictly sinking behavior, according to the respective Monotonic settlement-rotation curves.

The above conclusions can be verified in **Figure 4.9**, which displays, for cyclic loading Type III, the evolution of settlement for a given displacement amplitude and all types of soil improvement. These charts show that for smaller amplitudes all models accumulate settlement, but there is a clear quantitative difference between the three models of z/B=0.5, 1 and homogeneous dense sand, and the other two models, which display two times the settlement of the former ones. However, as the amplitude of the imposed displacement increases, the two areas of differing behavior start to become more emphatic. The two “loose models” continue to accumulate settlement even so at an increase rate, while the three “stiff” models demonstrate almost no extra settlement for larger amplitude cycles, meaning that uplift dominates their behavior. This behavior could be attributed to the fact for large displacements, the soil improvement in the three “stiff” models plays an

important role in the stiffness and the bearing capacity of the soil, due to the fact that foundation uplift reduces the contact area and so the depth at which stresses are transmitted.

FIGURES

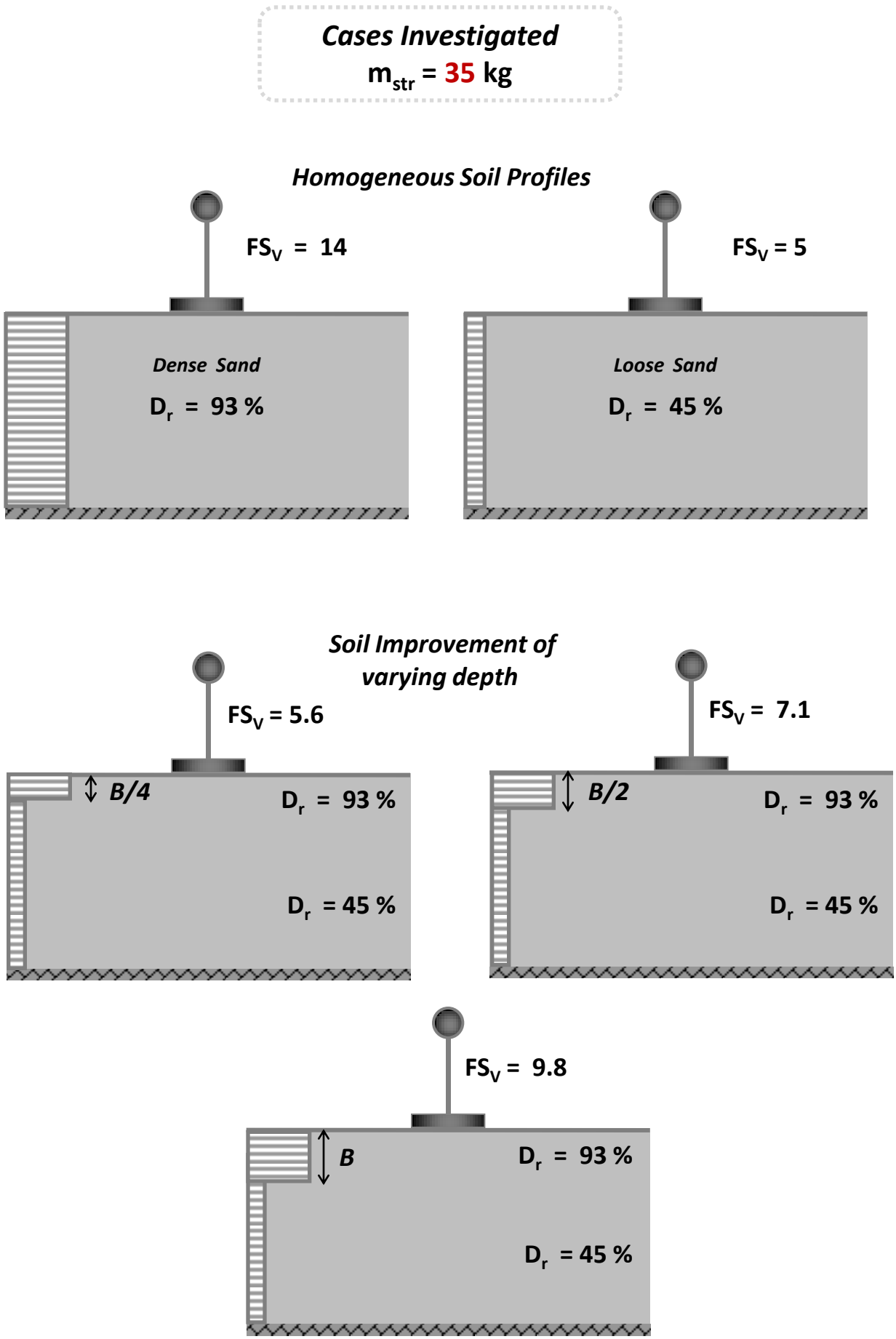

Figure 4.1. Schematic illustration of soil–foundation–superstructure systems studied. The structural mass is m_{str} **= 35 kg**.

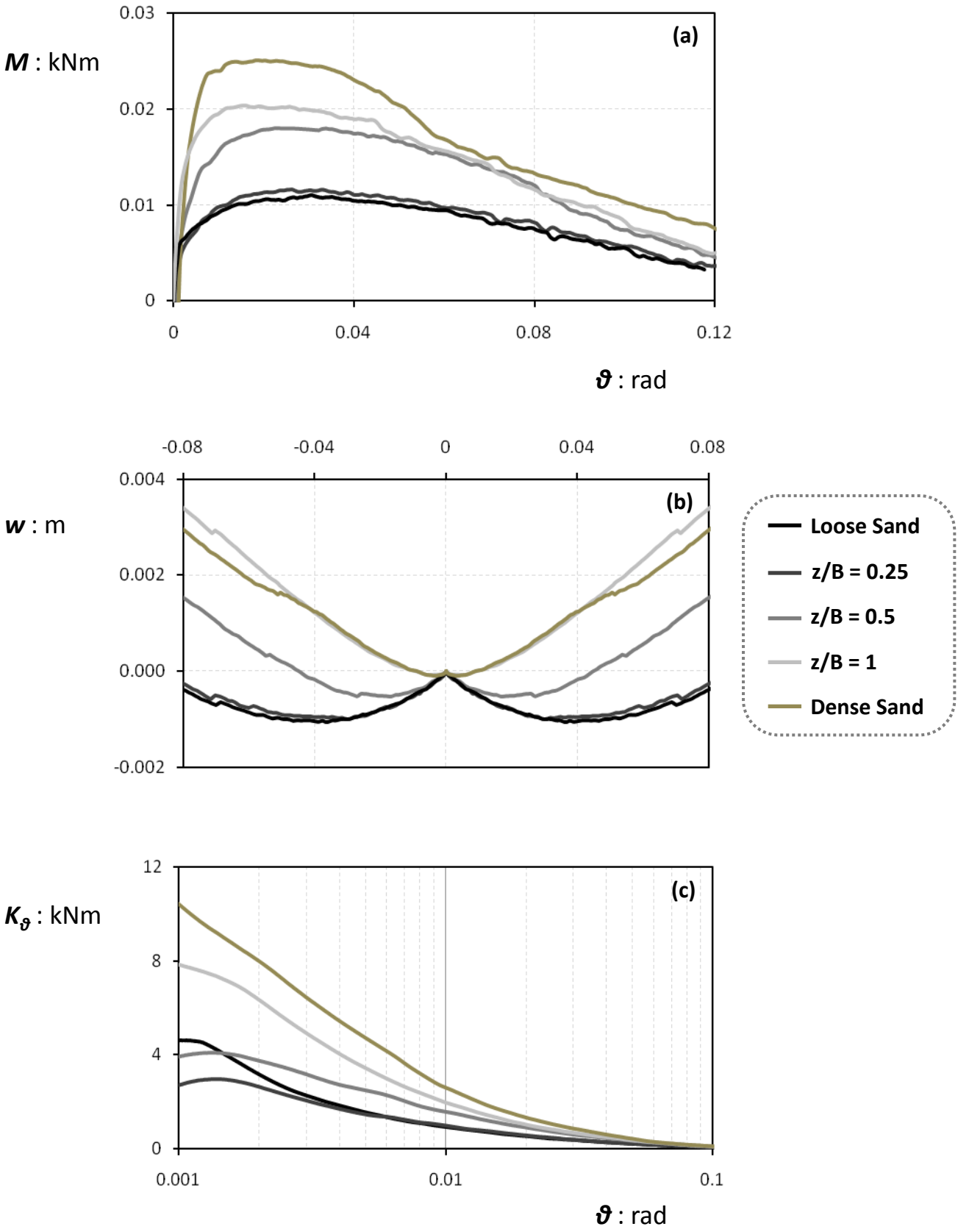

Figure 4.2. **(a)** Moment–rotation curves, **(b)** settlement–rotation curves, **(c)** rotational stiffness curves derived from monotonic pushover tests for systems lying on homogeneous and two-layered soil deposits. The structural mass is m_{str} **= 35 kg**.

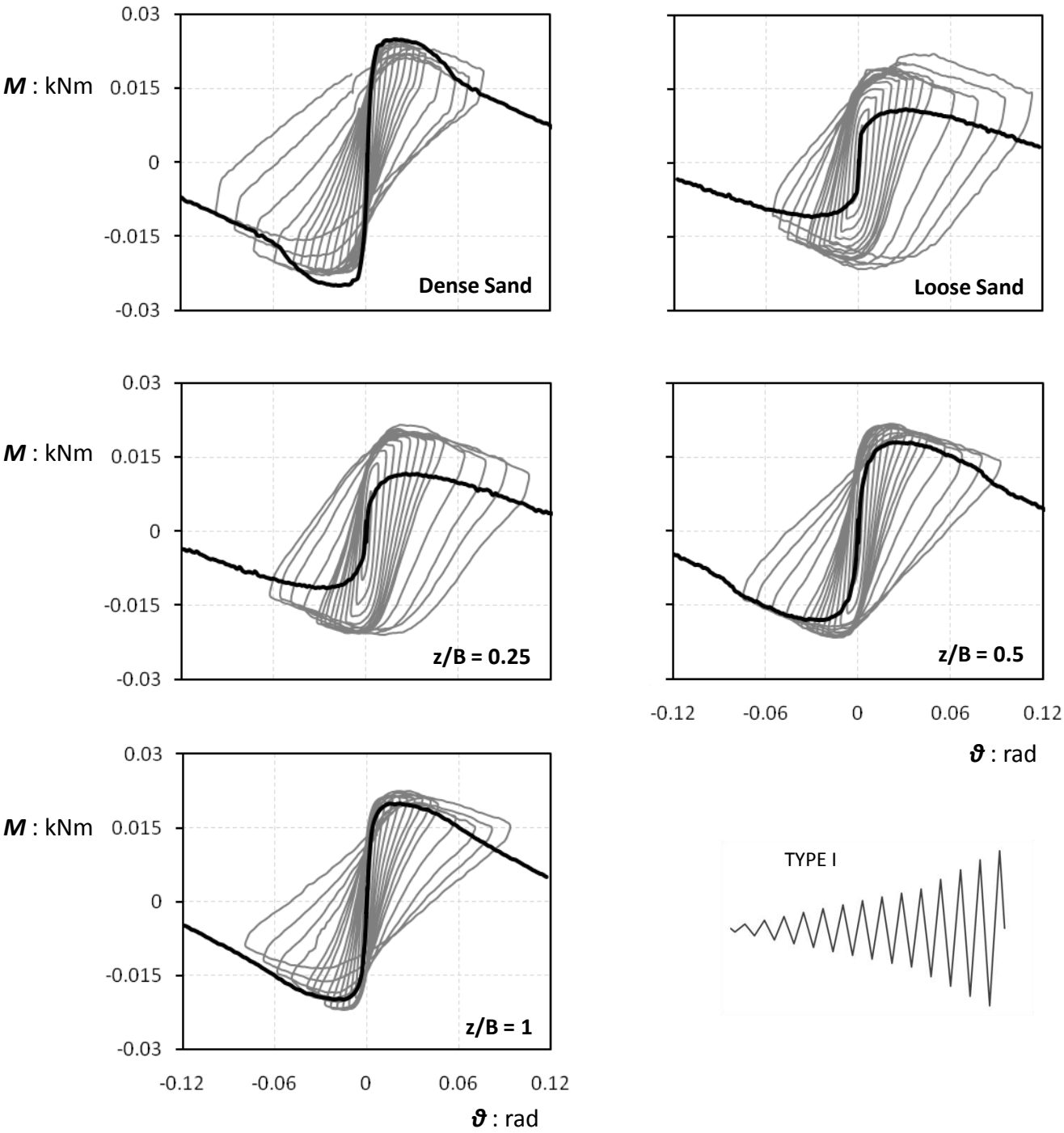

Figure 4.3. Moment–rotation curves derived from slow cyclic pushover tests (**TYPE I**) for systems lying on homogeneous and two-layered soil deposits. The structural mass is **m_{str} = 35 kg**.

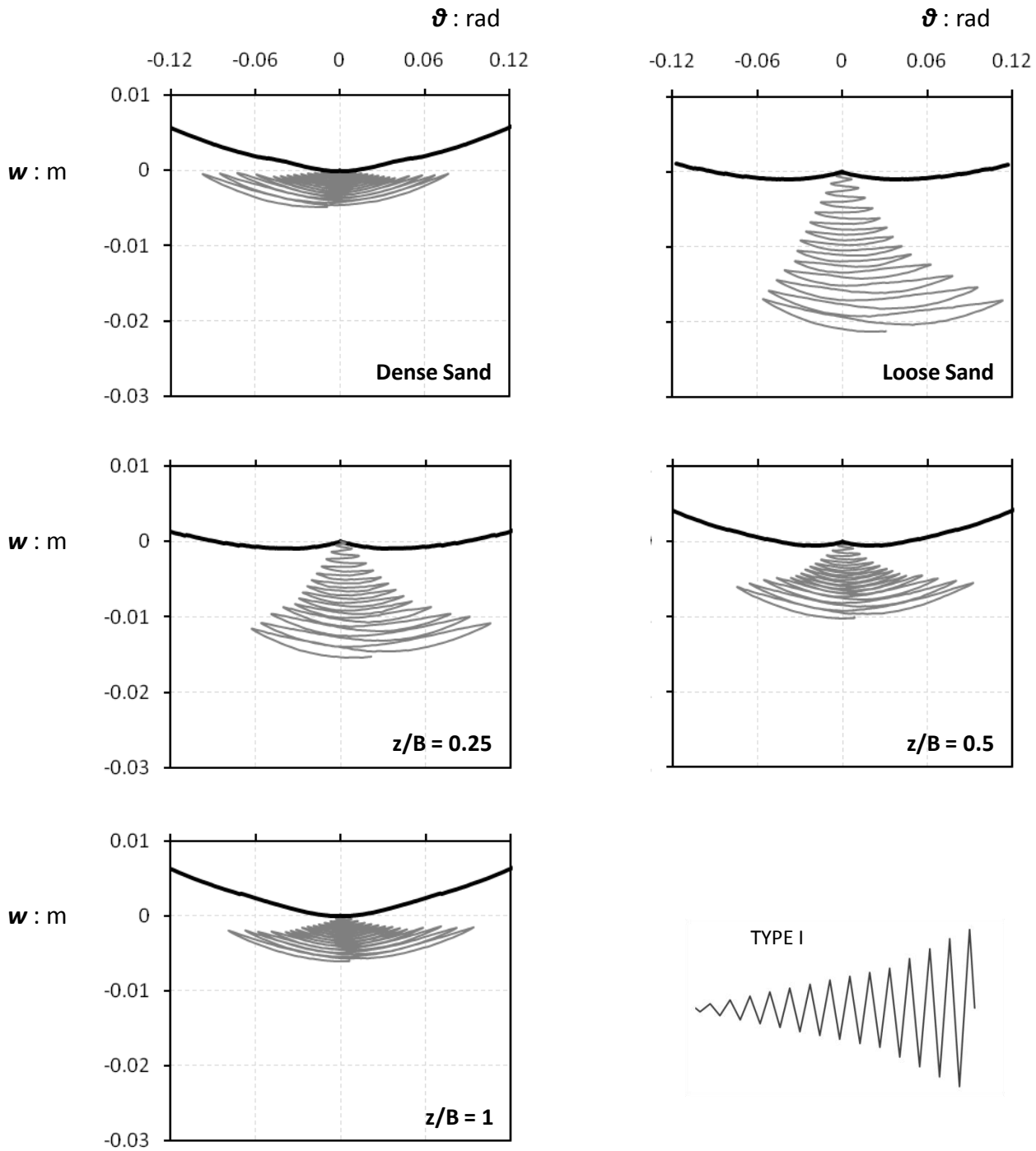

Figure 4.4. Settlement–rotation curves derived from slow cyclic pushover tests (TYPE I) for systems lying on homogeneous and two-layered soil deposits. The structural mass is $\mathbf{m_{str} = 35\ kg}$.

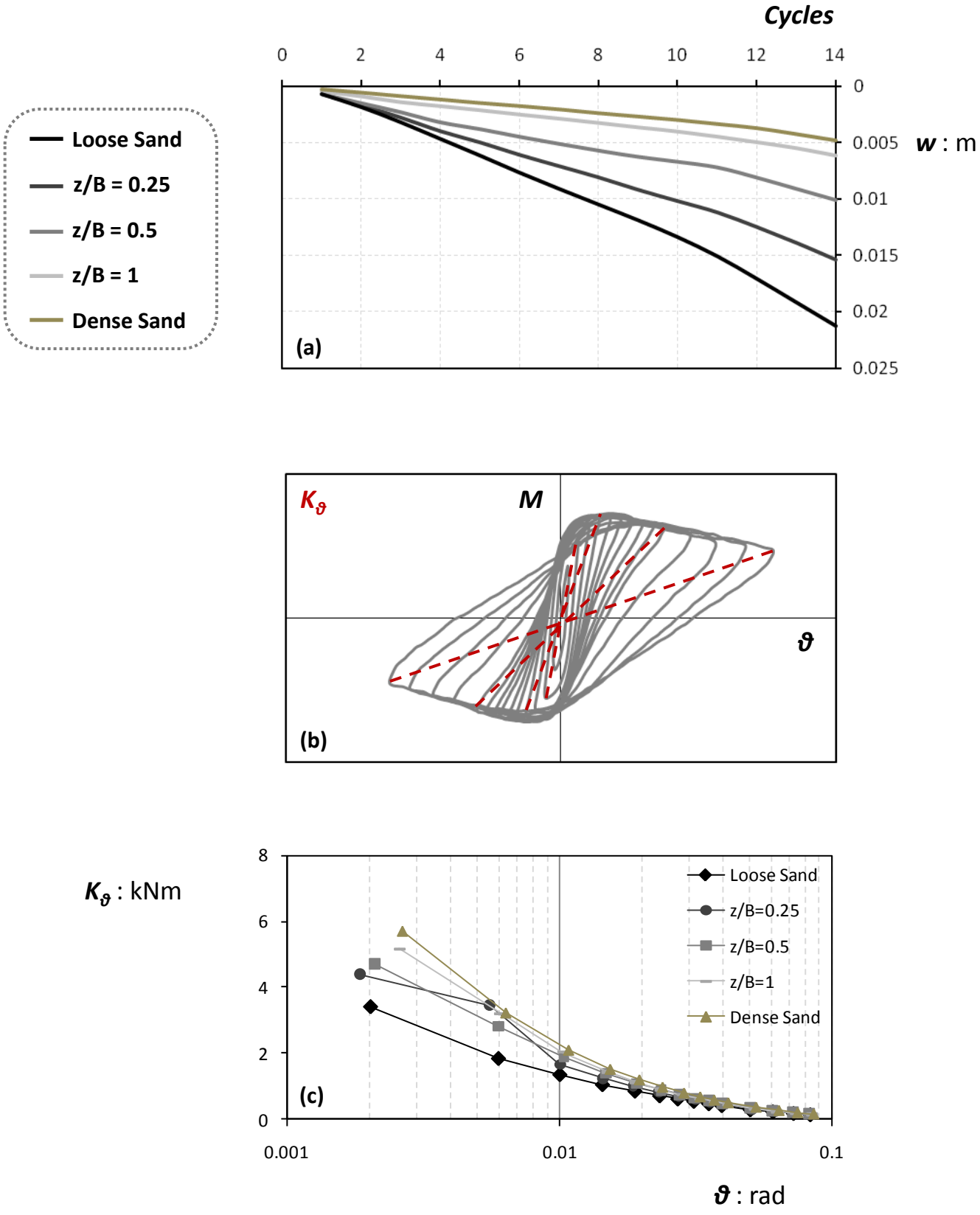

Figure 4.5. (a) Accumulation of settlement per cycle **(b)** schematic illustration of rotational stiffness computed for cyclic loading and **(c)** rotational stiffness curves derived from slow cyclic pushover tests (**TYPE I**) for systems lying on homogeneous and two-layered soil deposits. The structural mass is $\mathbf{m_{str} = 35\ kg}$.

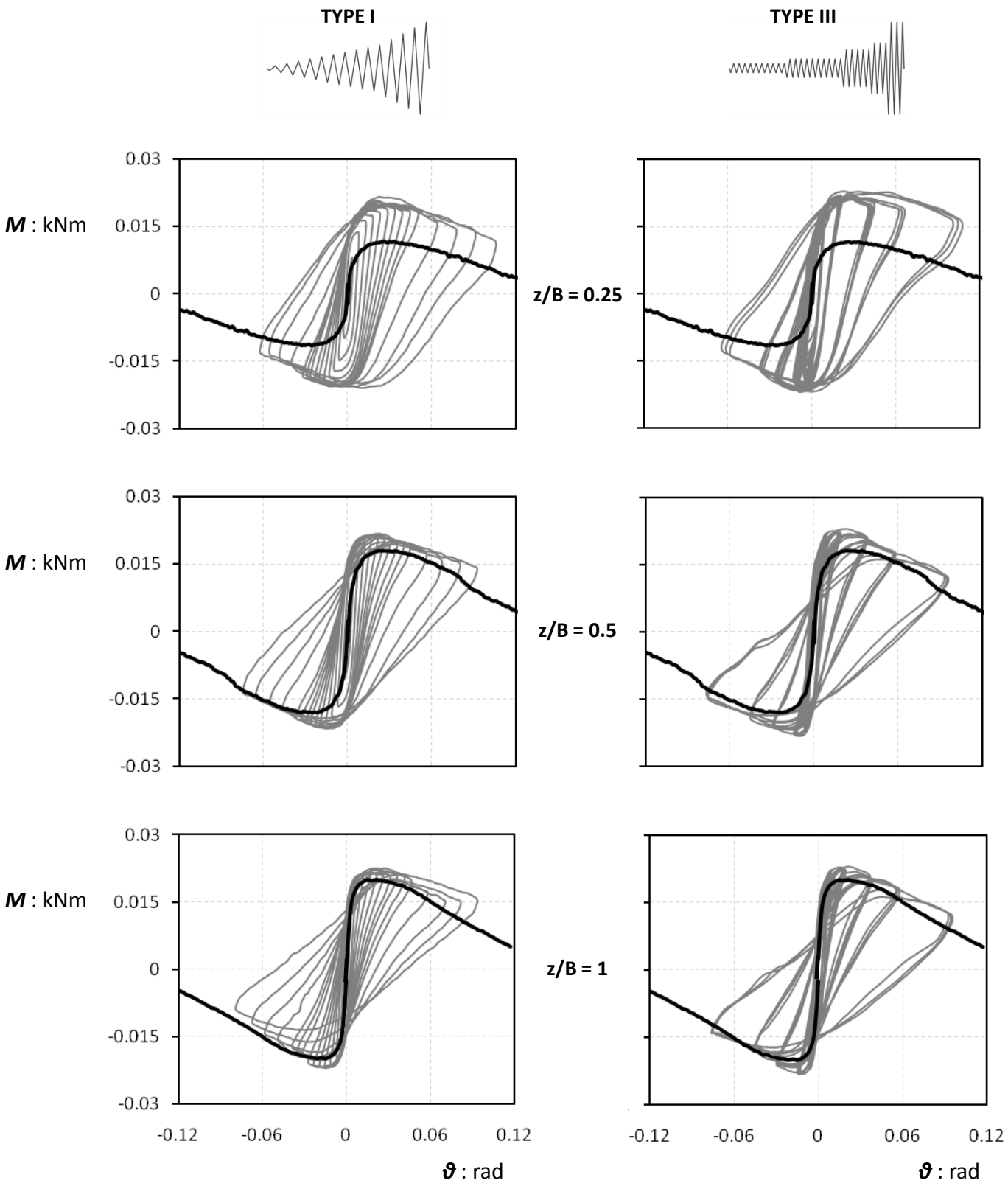

Figure 4.6. Moment–rotation curves derived from slow cyclic pushover tests (TYPE I & TYPE III) for systems lying on two-layered soil deposits. The structural mass is m_{str} = 35 kg.

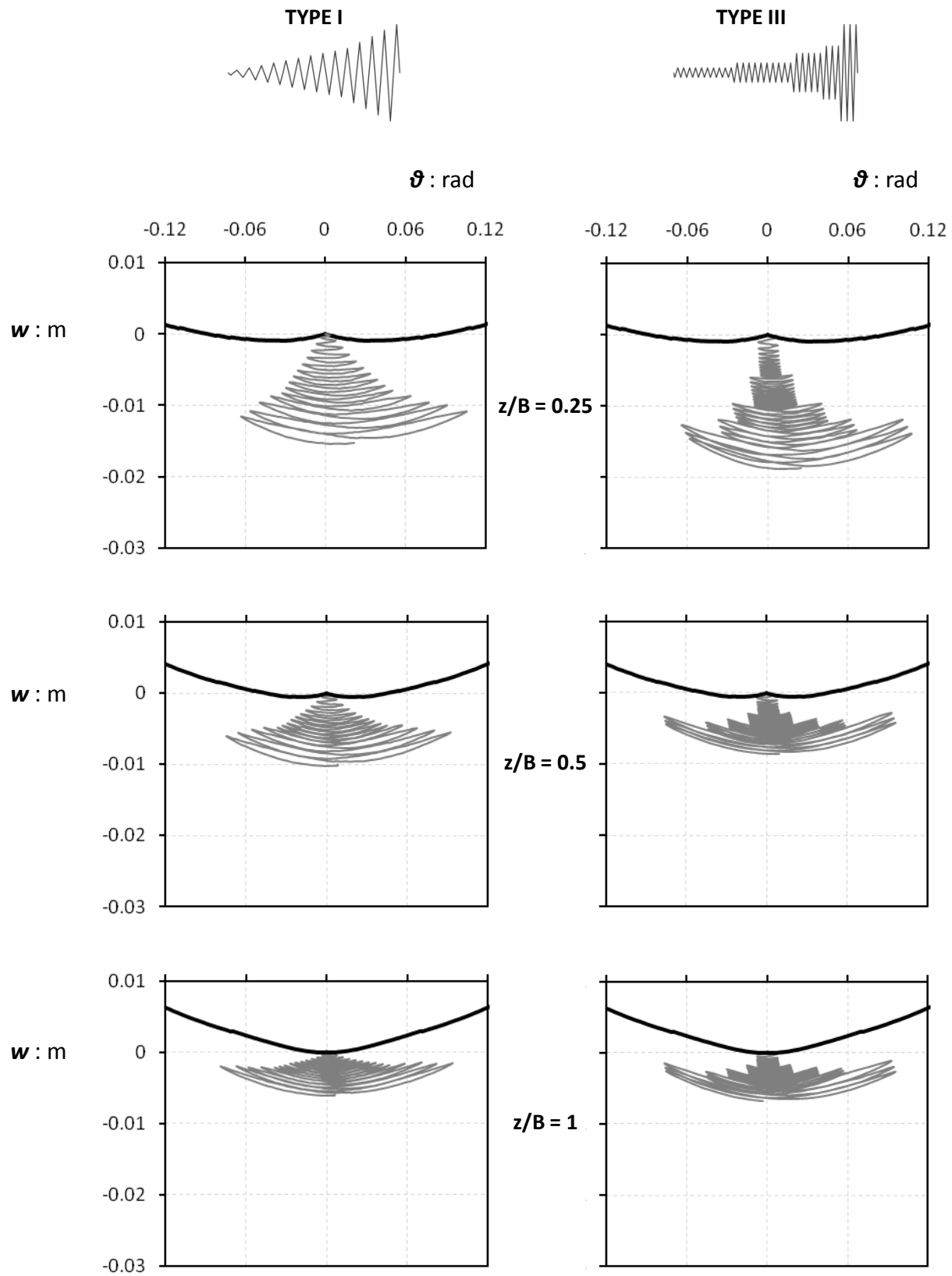

Figure 4.7. Settlement–rotation curves derived from slow cyclic pushover tests (TYPE I & TYPE III) for systems lying on two-layered soil deposits. The structural mass is m_{str} = 35 kg.

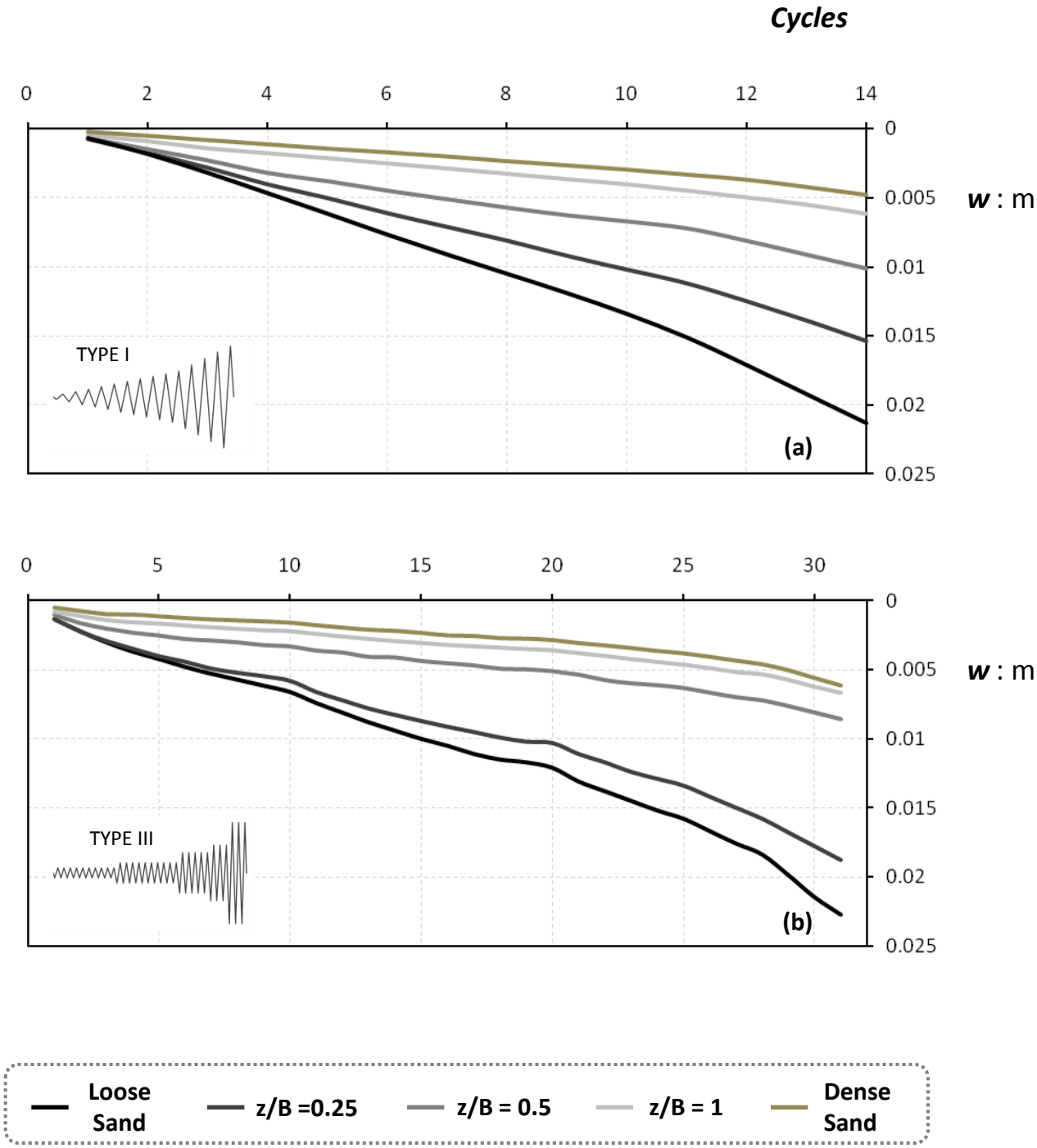

Figure 4.8. Accumulation of settlement with respect to the number of cycles during slow cyclic pushover tests **(a)** TYPE I and **(b)** TYPE III, for systems lying on homogeneous and two-layered soil deposits. The structural mass is $\mathbf{m_{str} = 35\ kg}$.

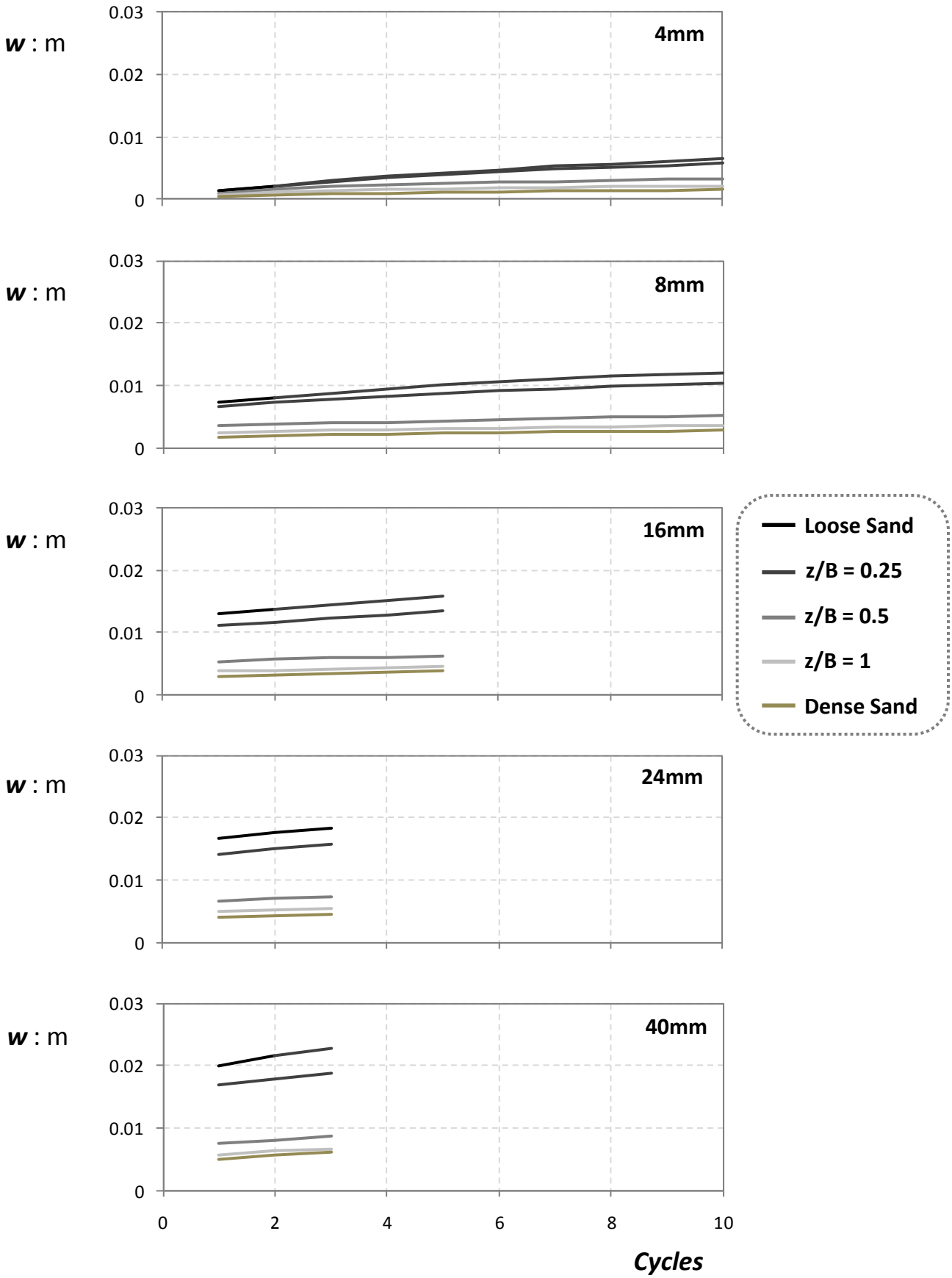

Figure 4.9. Evolution of settlement with respect to the number of cycles for different displacement amplitudes imposed during slow cyclic pushover tests (**TYPE III**) for systems lying on homogeneous and two-layered soil deposits. The structural mass is $\mathbf{m_{str} = 35\ kg}$.

Chapter V:

Shallow Soil improvement : 100kg Model Investigation

5.1 Introduction

This chapter examines the behavior of a relatively heavy structure subjected to horizontal pushover tests and how shallow soil improvement could help improve its response and alleviate the general problems derived from foundation rocking. The reason this model was chosen is because very high factors of safety, of the order of 10 or more are not always required by design standards and most of the time are not economically feasible. As a result, it would be interesting to see the effects of shallow soil improvement in a building with relatively low FS_v meaning that the rocking performance would be mainly sinking dominated from the start.

After consideration, it was decided that the two homogenous profiles to be used would be dense sand (D_r = 92%) and sand of medium relative density (D_r =65%) which display respective FS_vs of 5 and 2.6. an overview of the case investigate is displayed in **Figure 5.1**. The depths of soil improvement to be examined would be z/B=0.5 and z/B=1. Contrary to the 35kg model, the crust with z/B=0.25 was not examined because it displayed virtually no difference from the model lying on homogenous sand of Medium density and the improvement was deemed inadequate.

5.2 100kg Foundation

Monotonic Loading

For the same reasons as before, the models were first subjected to Horizontal monotonic loading. The results are displayed in **Figure 5.2**.

The first chart shows a comparison in terms of moment-rotation. As far as ultimate moment achieved is concerned, it is again obvious that the improvement in soil quality gives proportionally larger values, although the difference is not as large as for the model in the previous chapter, mainly due to the fact that all models are closer to FS_v=2, which displays the highest bearing capacity. Regarding the overturning angle displayed, there seems to be a small trend in increase of the angle with an increase in the depth of the soil improvement but generally, this difference is relatively small, compared to the change in the FS_v. This might be attributed to the fact that for such small FS_v values, soil failure dictates the overturning angle and as such, since all structures are relatively heavy, they display similar θ_u.

The second chart displays the Monotonic Loading in Terms of settlement-rotation. It is obvious here that the increase in the depth of soil improvement reduces the rotation amplitude where sinking is realized. For small amplitude of cycles, the 4 curves almost fit, because the effect of the soil improvement is negligible due to the fact that the stresses extend to a very large depth, as

mentioned before, however as the contact area is reduced, the improved soil plays an increasingly larger role in the response of the system. This is even more clear for the cases of Dense homogenous sand and z/B=1, where, for medium to large rotations, the two curves are almost parallel to each other, with their difference being the extra settlement the latter one has accumulated in small rotations. Same is true for the cases of Homogeneous Sand of medium density and model with z/B=0.5. For small amplitudes, the two lines are matching, whereas for larger ones, there is an increasing difference in settlement accumulated.

In terms of secant rotational stiffness with respect to rotation, similar behavior to the 35kg model is observed. There is an increase in rotational stiffness with the increase in the depth of the soil improvement, with the exception of the model lying on the sand of medium density, which for small rotation displays a larger stiffness that the one with soil improvement and z/B=0.5. This, again, should be attributed in our inability to make accurate measurements in small rotations.

Cyclic Loading

Investigating the response of the four models subjected to slow cyclic lateral loading, the results seem similar to the ones analyzed in the previous chapter. **Figure 5.3** displays the comparison in terms of moment-rotation. All models display an almost identical Maximum moment for the same rotation

amplitude, especially for larger amplitudes where the overstrength has been mobilized in its total. As for the overstrength factor, again an increase in the safety factor reduces the ultimate moment achieved relative to the ultimate moment derived from the monotonic tests. Both systems with soil improvement demonstrate an overstrength factor somewhere in between the one displayed by the two models lying on homogeneous strata. Also considering the results from the previous chapter, it is safe to say that Ultimate moment capacity in cyclic tests is not dictated by soil quality, rather than foundation and superstructural properties. Finally, the loop shapes display a lot of similarities, which is something to be expected, considering the two homogeneous profiles do not demonstrate themselves striking differences, due to the FS_vs being close.

Moving on to settlement – rotation comparison, the results are shown in **Figure 5.4**. These charts show that qualitatively, the response of the systems investigated is similar, meaning the response is mainly dominated by sinking rather that foundation uplift. Due to this, all foundations display considerable settlement. However there is a striking difference in the absolute value of the settlement accumulated for each model, which can be justified by the monotonic curves shown in previous figure. It is shown that even for the shallower soil improvement of z/B=0.5, settlement is considerably reduced and moving even further to the model with improvement of z/B=1 provides an even more satisfying response, with the residual settlement more than halved, compared to the model lying on homogeneous sand of medium density. In fact

the model with z/B=1 displays a behavior much more similar to the one lying on homogeneous Dense sand stratum.

Load protocol comparison

For the same reasons as in the case of the 35kg superstructure, discussed in the previous chapter, the models are also subjected to loading protocol Type III.

Comparing the two models with soil improvement for the two different loading protocols, the results in terms of moment-rotation are shown in **Figure 5.5**. As in the previous chapters, for the same depth of soil improvement, the results for the two loading Types are similar. Comparing maximum moment achieved for cycles of the same amplitude, both loading types display the same values. In fact, as seen before, there is no degradation of either maximum moment or rotational stiffness regardless of the number of cycles of the same amplitude. This however, is not an entirely general assumption. Looking closely at the charts, for cycles of very small amplitude, Loading Type I does not mobilize the full moment capacity of the model, instead following the course of the monotonic backbone curve. Contrary to that, in Loading Type III and for small amplitudes, there seems to be a rapid mobilization of moment capacity after the first few cycles, which leads all the way to displaying considerable overstrength. This could be attributed to the fact that the extent of the overstrength is relative to the loading history. For Loading Type I, few or no

cycles precede, while in Loading Type III, Having a lot of cycles in the same amplitudes mobilizes the entirety of the bearing capacity. However, maximum overstrength does not vary at all for the two load types, so it is safe to say that there is an ultimate value that cannot be exceeded.

Figure 5.6 displays a comparison of the same models in terms of settlement – rotation. Loading protocol type III evidently displays more settlement compared to Type I, something that, as stated before, is generally expected. The relative increase in settlement is greater for the model with z/B=0.5. This is attributed to the fact in the amplitude of cycles imposed, the aforementioned model displays greater sinking, according to the results derived from monotonic loading. Another interesting note is that the biggest difference between the two models for cyclic Loading Type III seems to come from settlement for small amplitude cycles, whereas in cyclic loading Type I the increase is gradual. This may be attributed to soil densification. In Load Type III the small amplitude cycles are many in number, whereas in Load Type I the same effect happens for cycles of greater amplitude.

The similar results are derived from **Figure 5.7** showing the evolution of settlement with respect to the number of cycles. It is derived from the first chart that in term of total settlement, The model with z/B=1 almost matches the one lying on homogeneous dense stratum. On the other hand, for Loading Type III, the decrease of the residual settlement with respect to the increase of the depth of the improvement is gradual.

Figure 5.8 illustrates the accumulated settlement per cycle for Loading Type III and different displacement amplitudes imposed. As in the 35kg superstructure scenario, for small amplitudes of displacement, the four models demonstrate similar behaviors, due to the fact that there is no uplift and the stresses stretch deep in the soil stratum. However, in this case, for larger displacements, the performance does not vary greatly as in the case of the lightweight superstructure, investigated in the previous chapter. A tendency for two different areas to form in large amplitudes seems to exist, but due to the small FS_v uplift is only identified for very large, if any amplitudes. Due to that, all models demonstrate sinking behavior in most amplitudes and the response is similar.

FIGURES

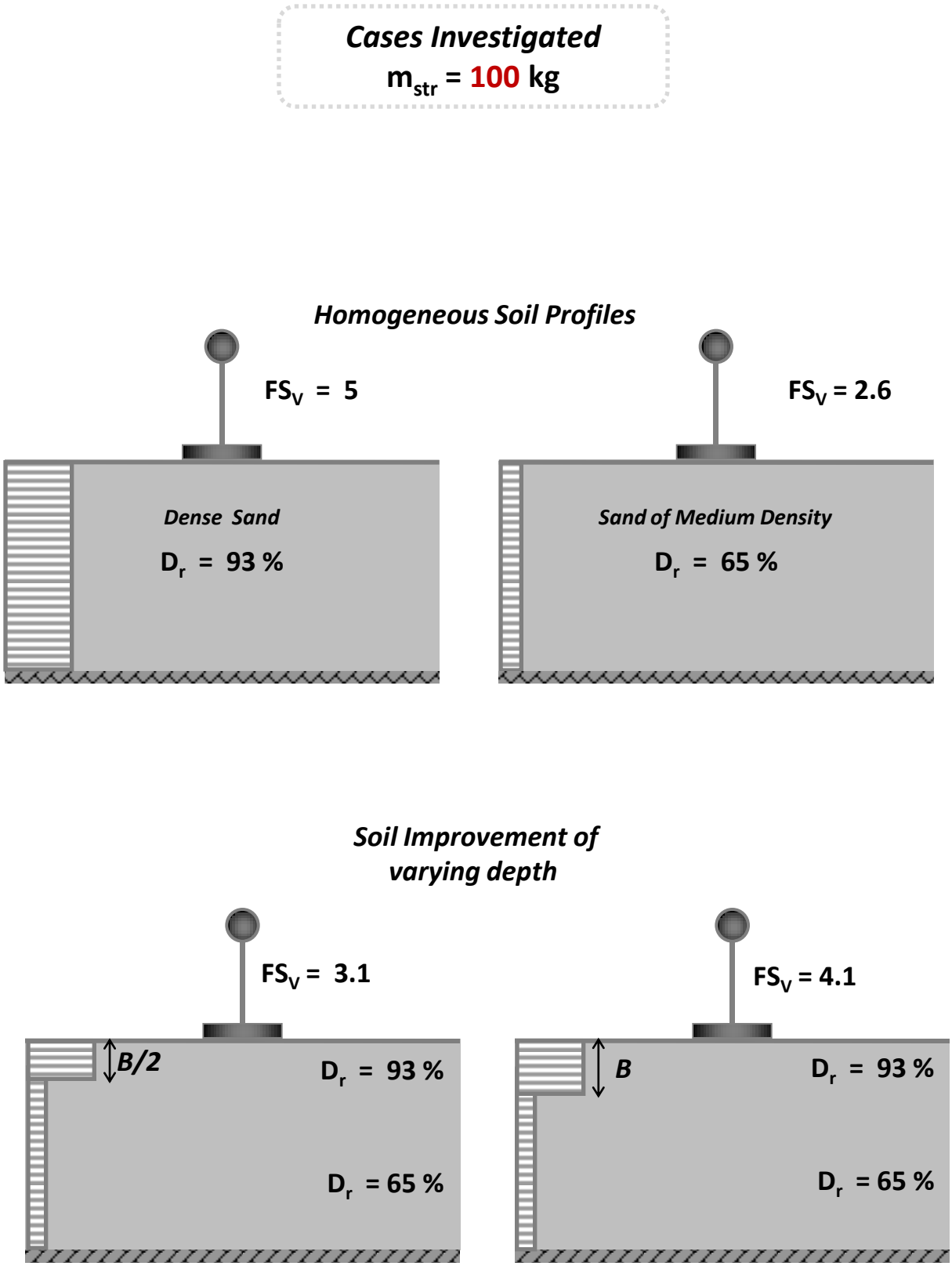

Figure 5.1. Schematic illustration of soil–foundation–superstructure systems studied. The structural mass is $\mathbf{m_{str}}$ **= 100 kg**.

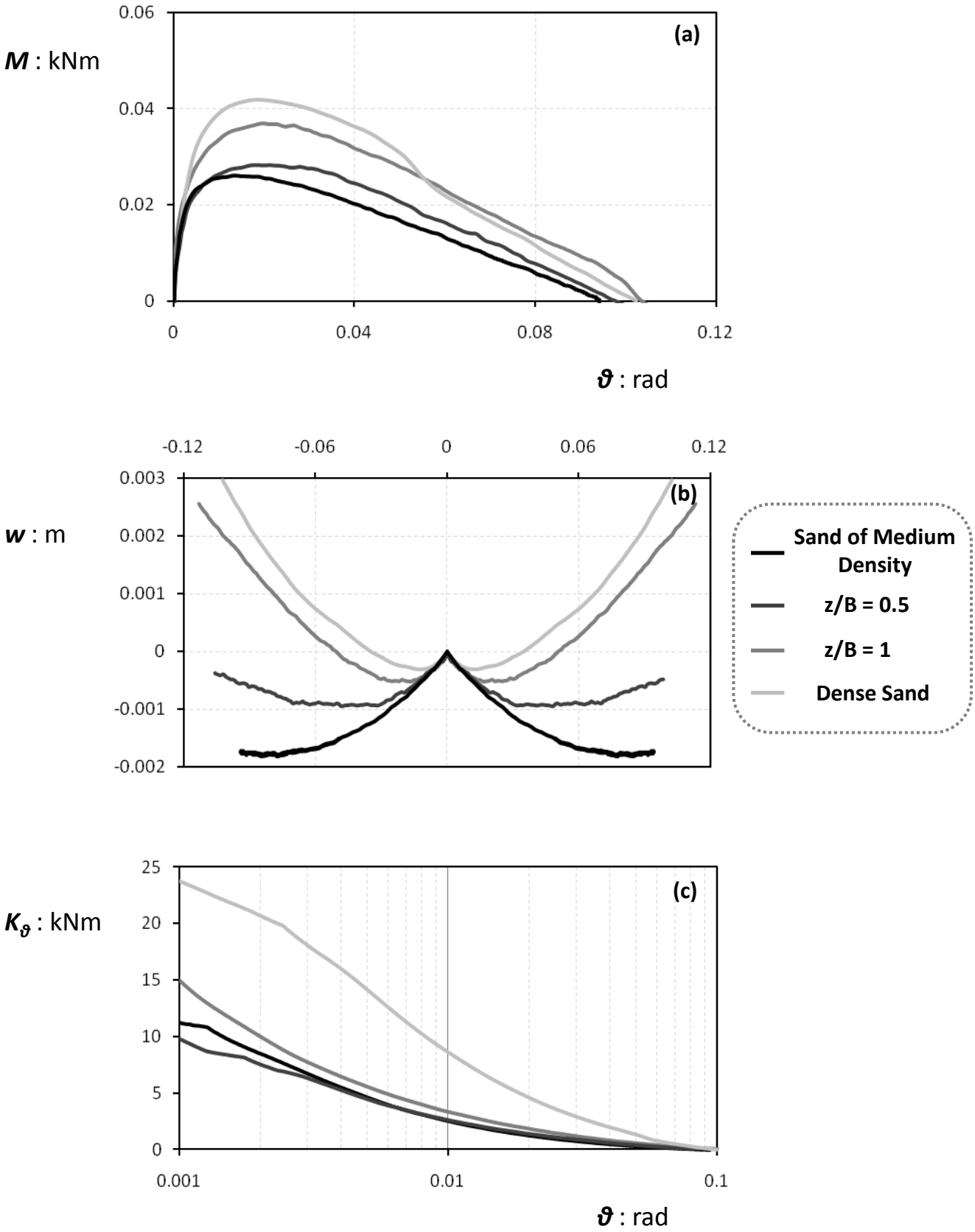

Figure 5.2. (a) Moment–rotation curves, **(b)** settlement–rotation curves, **(c)** rotational stiffness curves derived from monotonic pushover tests for systems lying on homogeneous and two-layered soil deposits. The structural mass is m_{str} **= 100 kg**.

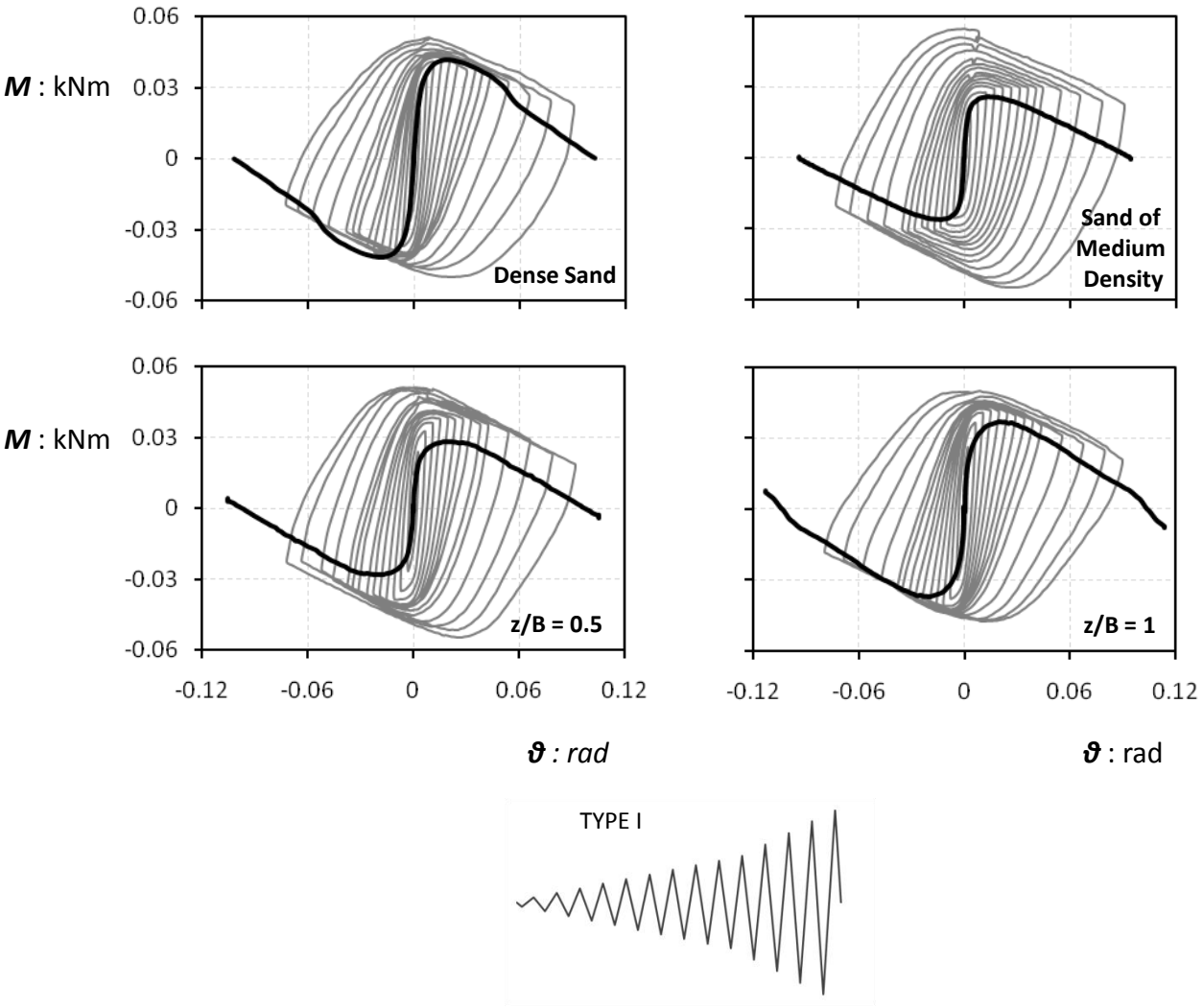

Figure 5.3. Moment–rotation curves derived from slow cyclic pushover tests (**TYPE I**) for systems lying on homogeneous and two-layered soil deposits. The structural mass is $\mathbf{m_{str} = 100\ kg}$.

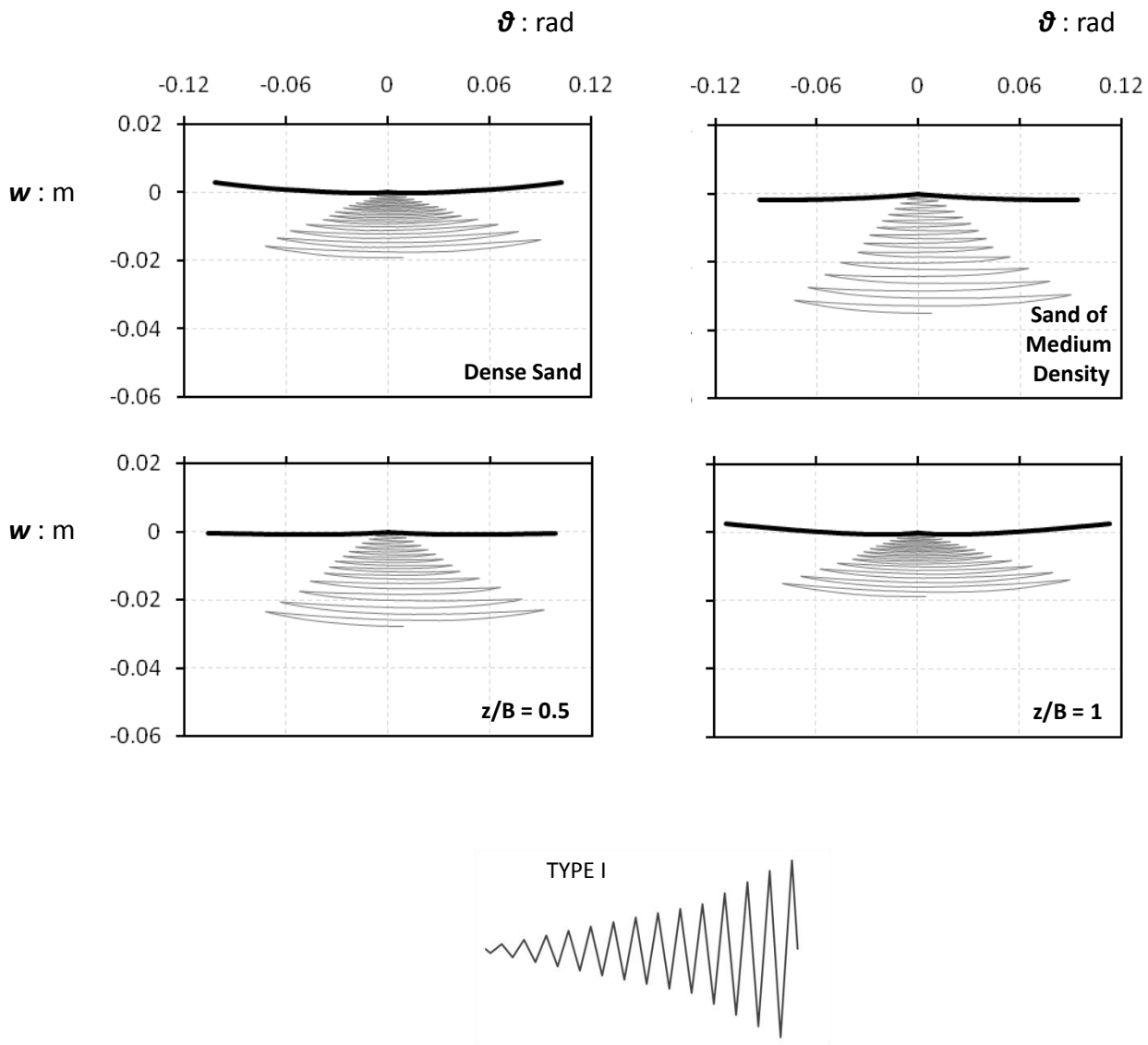

Figure 5.4. Settlement–rotation curves derived from slow cyclic pushover tests (**TYPE I**) for systems lying on homogeneous and two-layered soil deposits. The structural mass is **m_{str} = 100 kg**.

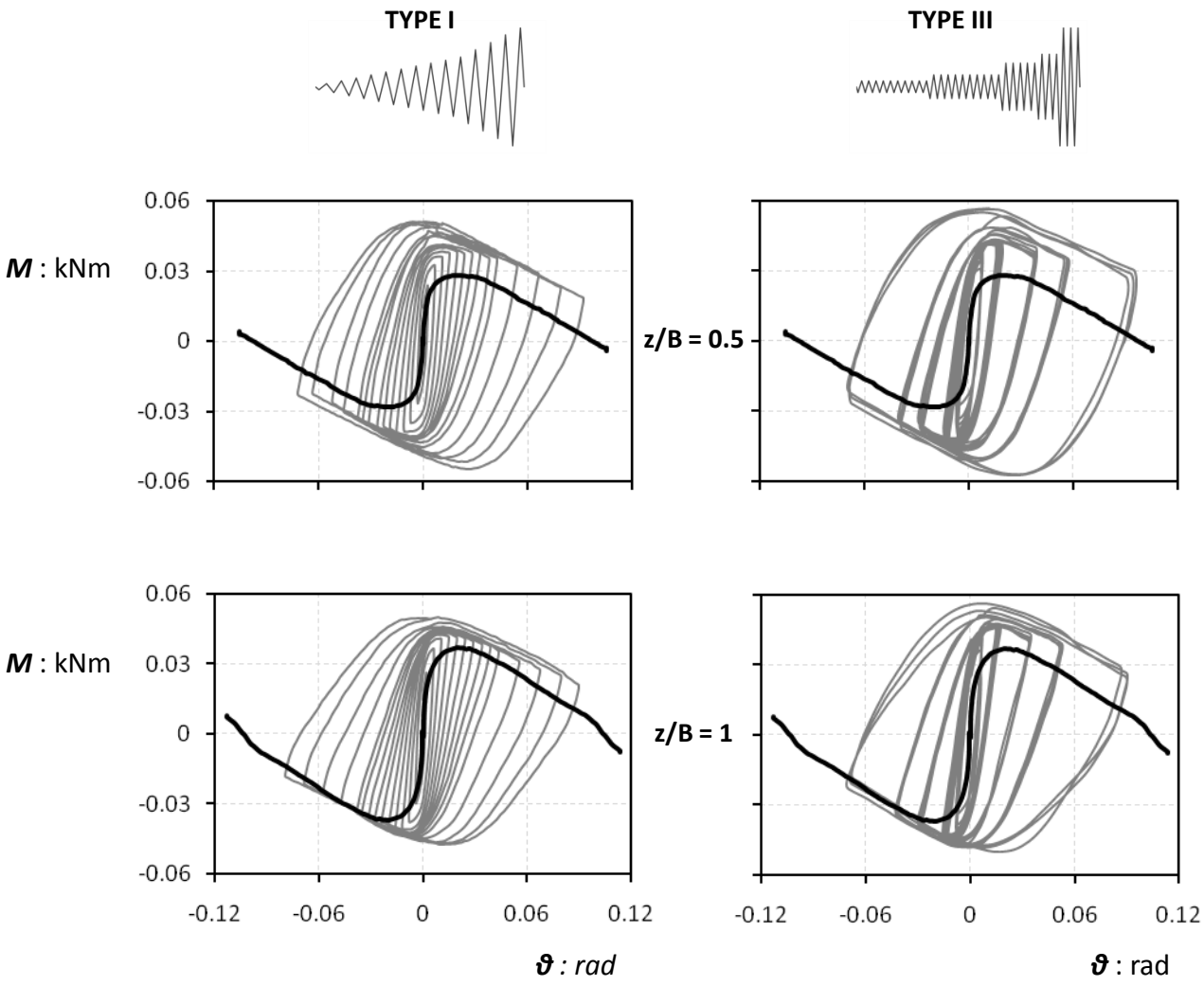

Figure 5.5. Moment–rotation curves derived from slow cyclic pushover tests (TYPE I & TYPE III) for systems lying on two-layered soil deposits. The structural mass is $\mathbf{m_{str}}$ **= 100 kg**.

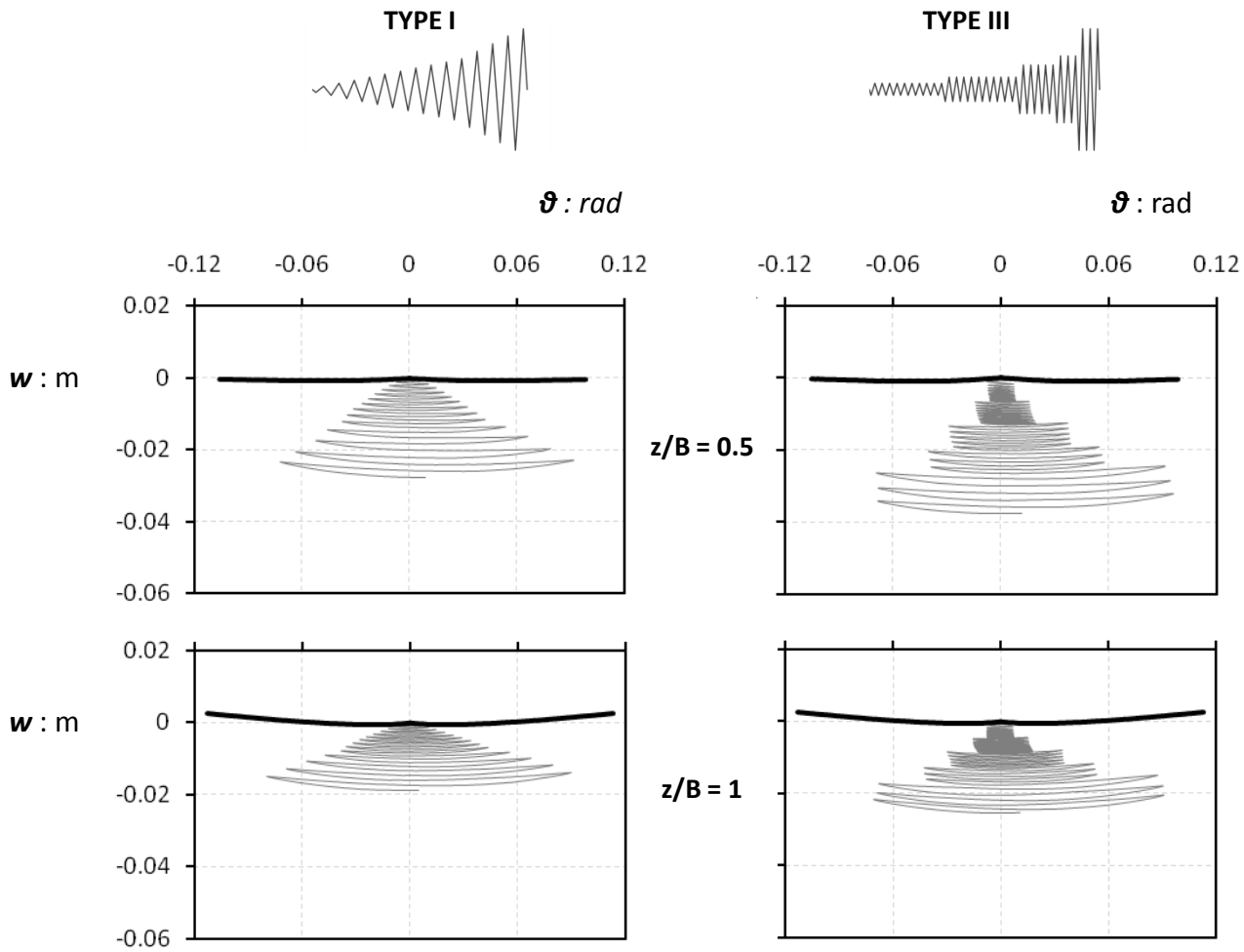

Figure 5.6. Settlement–rotation curves derived from slow cyclic pushover tests (TYPE I & TYPE III) for systems lying on two-layered soil deposits. The structural mass is $\mathbf{m_{str} = 100\ kg}$.

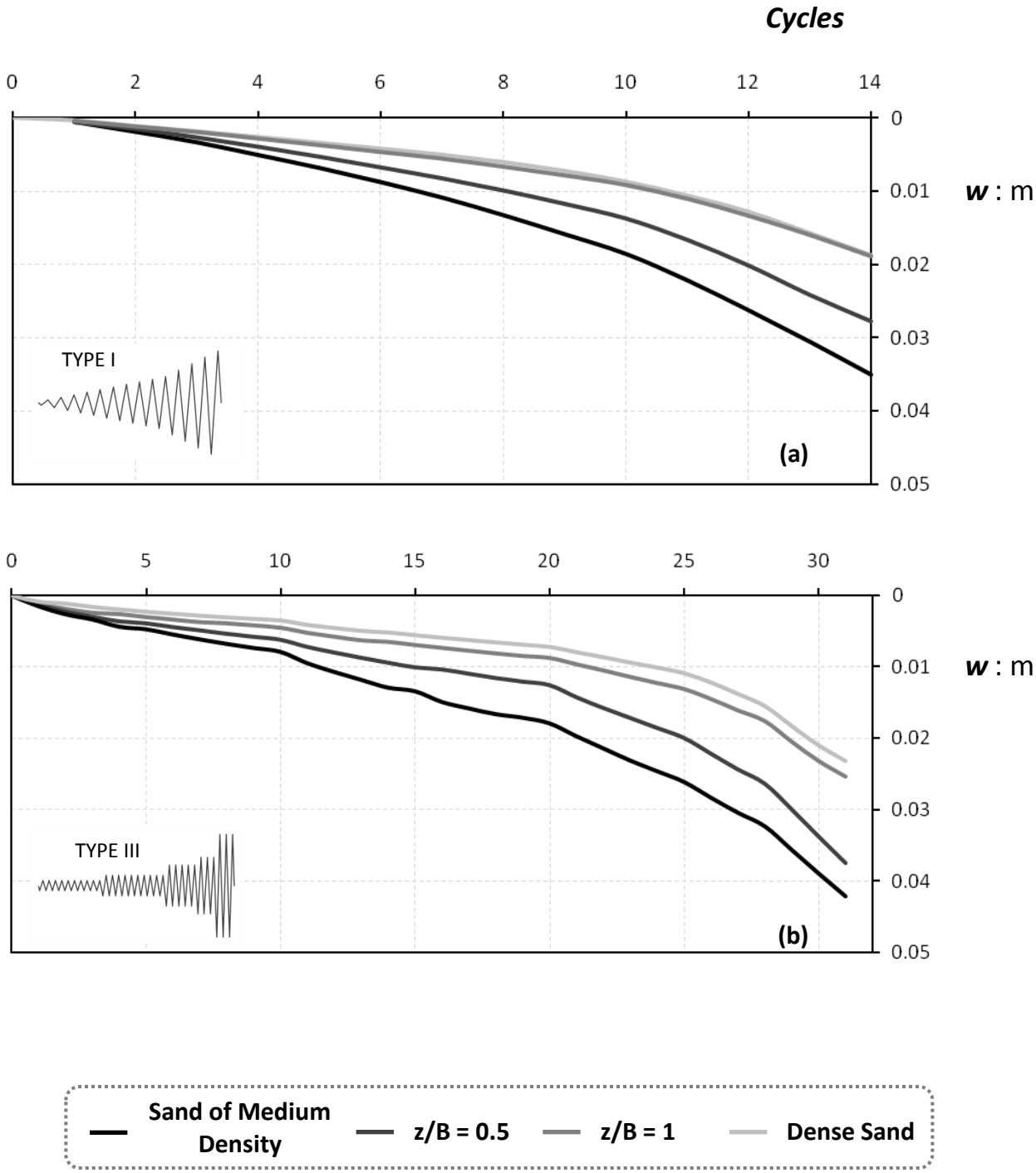

Figure 5.7. Accumulation of settlement with respect to the number of cycles during slow cyclic pushover tests **(a)** TYPE I and **(b)** TYPE III, for systems lying on homogeneous and two-layered soil deposits. The structural mass is **m_{str} = 100 kg**.

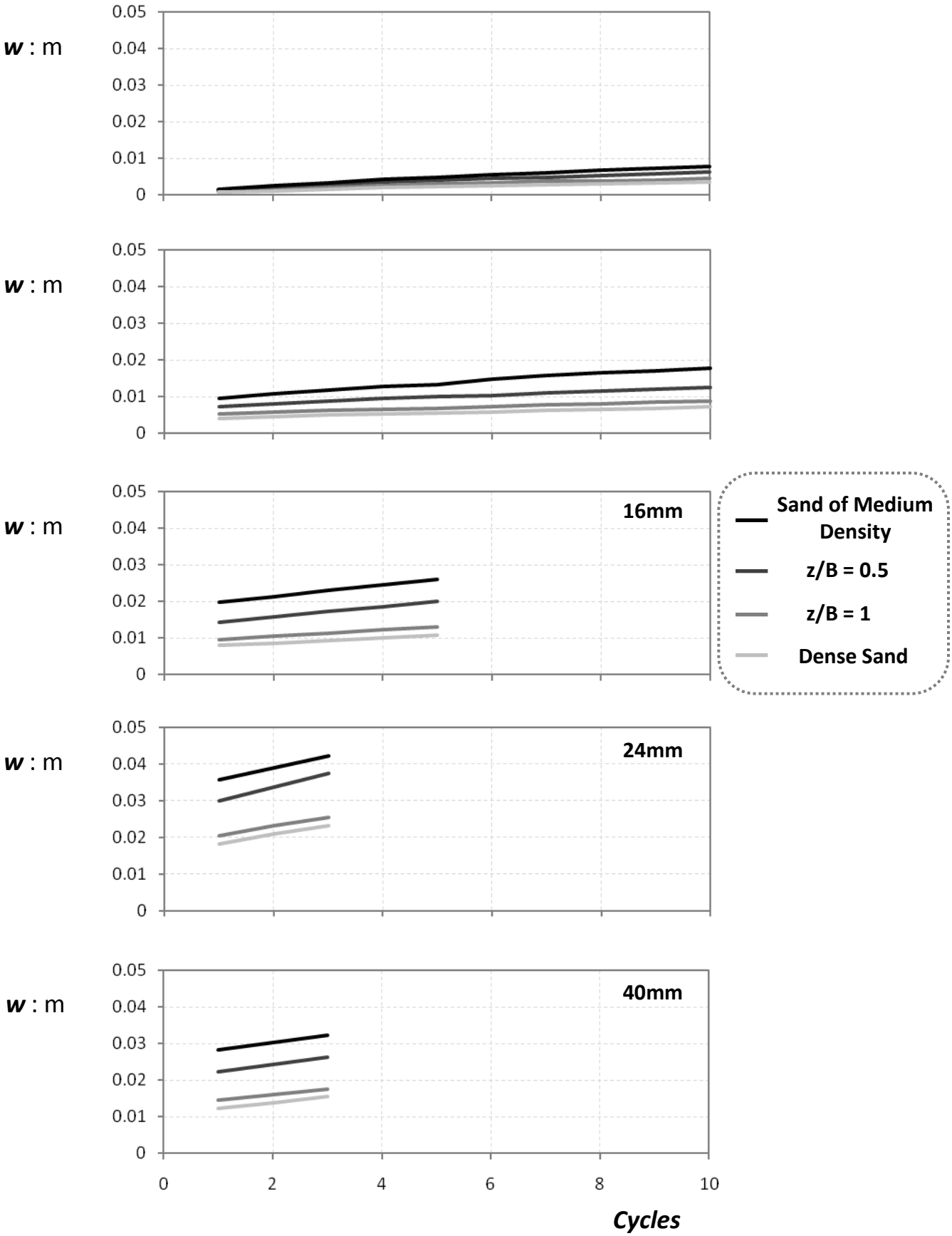

Figure 5.8. Evolution of settlement with respect to the number of cycles for different displacement amplitudes imposed during slow cyclic pushover tests (**TYPE III**) for systems lying on homogeneous and two-layered soil deposits. The structural mass is m_{str} = 100 kg.

CHAPTER VI:

CONCLUSIONS – FURTHER INVESTIGATION

5.1 Conclusions

This study investigated the response of a single degree of freedom oscillator lying on sand stratum and subjected to horizontal pushover tests. The results of this experimental investigation can be organized into several axes.

Homogeneous stratum

First, comparing structures lying on sand of the same density and differing in superstructural mass, which leads to different FS_v, the following conclusions can be extracted:

- Larger FS_v leads to larger overturning angles
- In the case investigated, smaller FS_v leads to larger ultimate bearing capacity. This of course is true only for the range of FS_vs investigated. One would expect a maximum to exist for FS_v of around 2.
- The overstrength factor for the cyclic tests is reduced as The FS_v rises.

- Contrary to results derived from experiments and analyses on clay [citation], a dominantly uplifting behavior for models lying on sand is clear only for very large Factors of Safety.

- All the results extracted in terms of bearing capacity are in accordance with the failure envelopes derived by Butterfield and Gottardi [Cit]. Especially when taking into account the scale effects, the difference is negligible.

- In terms of settlement, higher FS_v leads to smaller accumulated settlement, especially for larger amplitudes of imposed displacement.

- Rotational stiffness is totally dependent on the confinement stresses for the case of sands, so the heavier the model and consecutively the lower the FS_v, the higher the rotational stiffness.

Comparing Structures of same superstructural mass lying on sand strata of different relative density D_r, resulting in different FS_v, the following can be concluded:

- Higher D_r leads to higher Ultimate moment M_u.

- Change of FS_v from 5 to 2.6 (100kg mass case) does not have a serious effect of the rocking response of the system especially for cyclic loading, whereas a change of FS_v from 5 to 14 results in a dominantly uplifting behavior.

Comparing Structures of the same mass lying on the same homogeneous soil stratum but subjected to different loading protocols, it was shown from the tests that:

- Generally, more cycles lead to more residual displacement.
- Bearing capacity for a given amplitude does not vary with load history, as long as a certain number of cycles have been already imposed so the systems develops full overstrength.
- The overstrength factor does not vary with the change in the load protocol
- Rotational stiffness does not seem to be affected by the number of cycles of the same displacement.

Comparing models with the same FS_v, lying on sand strata of different relative density D_r, the results derived from the tests show that:

- Obviously, Higher D_r leads to higher ultimate capacity M_u.
- Overturning angle, θ_u is larger for the model with the higher D_r. However this conclusion is not definite because, as previously stated, the Slenderness ration differs to a small extent, from one model to the other.
- Higher D_r leads to smaller residual displacements. However this is true only for the number of cycles we investigated. Tests show that there is a tendency for the two models to reach a limit state where, the more cycles

are imposed, the lesser the difference in accumulated settlement between them.

Shallow Soil Improvement

The primary scope of this investigation was to experimentally test and evaluate the concept of shallow soil improvement. To this end, the results derived from the tests, in the case of the model with a mass of m=35kg, show that:

- Ultimate moment M_u in monotonic loading is higher for higher ratios of z/B. This is not true however for cyclic loading. After a number of cycles imposed, all models reach the same ultimate Moment, which does not seems to vary after that point.
- As the z/B ratio rises, the models demonstrate an increasingly more uplift-dominated behavior, both in monotonic and cyclic loading.
- Rotational stiffness for both monotonic and cyclic loading is larger for larger ratios of z/B, with small exceptions mainly attributed to experimental flaws. The degradation of rotational stiffness with respect to the reduction in z/B ratio is smooth.

Comparing the same models in terms of load protocol imposed, the results show that:

- There is no difference between the load types in terms of Ultimate Moment achieved for a certain amplitude of displacement.
- Residual settlement does not have a general tendency with respect to the z/B ration for the two load types investigated. Different ratios show smaller, larger or practically the same settlement for the two Load Types.
- For Load Type III, The difference is settlement between models with different z/B ratio develops for medium and large amplitudes of imposed displacement.

For the case of the m=100kg model, the results are generally similar. That is to say:

- Ultimate moment is again relative to the ratio z/B for monotonic loading, but almost indifferent to it for cyclic loading.
- In contrast, overturning angle does not seem to differ so much as in the previous scenario, with all models demonstrating similar values.
- Again, uplift prevails over sinking as the z/B ratio increases.
- Rotational stiffness increases with the increase of the z/B ratio.
- Settlement increases gradually as the z/B ratio is reduced.
- Comparing the two Load protocols, settlement increases for Load protocol Type III, contrary to the case of the Lightweight structure.

- Again, in contrast with the lightweight model, the increase in settlement is gradual for all displacement amplitudes imposed and not focused on certain amplitudes.

5.2 Further investigation Proposed

This study investigated to some extent the effectiveness of shallow soil improvement on the rocking response of shallow foundations. While not totally complete, it shed some light as to whether this concept is useful. To further investigate the concept, it is very important to conduct further work.

The target of this project is to assess the performance of soil-foundation-superstructure system during EARTHQUAKE loading. Consecutively, nothing about this work would have any meaning if the necessary shaking table experiments are not conducted. It is imperative that the shaking table tests be commencing imminently, so that we can verify the results derived from this work.

A very important issue that is worth further investigation is the effect load history has on the response of the structure. This study showed that different load protocols make the structure behave differently. Further studies should focus on standardizing to some extent the load protocols say, using the

same number of cycles with different amplitude or the same amplitude with different loading history.

Another point that is of great importance is to investigate how the scale effects affect the performance of the model. This, to some extent was done in this work with the included comparison to the tests conducted at PWRI. However, the results can only be interpreted qualitatively, so further tests are needed, either large scale or using a centrifuge.

Another big step towards realizing this concept is to abandon the idea of a rigid elastic structure and move towards a more “real” one, with finite stiffness and capacity. Besides, the point of the whole “new design philosophy” is to guide failure to the soil elements instead of the superstructure, in cases of large shaking. This can only be evaluated if the superstructure CAN fail; otherwise it is just an ideal scenario.

CHAPTER VII:

BIBLIOGRAPHY

FEMA 356, (2000), *Prestandard and Commentary for the Seismic Rehabilitation of Buildings*.

Paolucci, R, & Pecker, A., (1997) "Seismic bearing capacity of shallow strip foundation on dry soils", *Soils and Foundations*; Vol. 37(3), pp. 95-105.

Pecker, A, (1998), "Capacity Design Principles for Shallow Foundations in Seismic Areas", *Proc. 11th European Conference on Earthquake Engineering*, A.A. Balkema Publishing.

Pecker, A, (2003), "A seismic foundation design process, lessons learned from two major projects : the Vasco de Gama and the Rion Antirion bridges", *ACI International Conference on Seismic Bridge Design and Retrofit*, University of California at San Diego, La Jolla, USA.

Gazetas, G., Apostolou, M., and Anastasopoulos, I. (2003), "Seismic Uplifting of Foundations on Soft Soil, with Examples from Adapazari (Izmit 1999, Earthquake)", *BGA Int. Conf. on Found. Innov., Observations, Design & Practice*, Univ. of Dundee, Scotland, September 25, pp. 37–50.

Anastasopoulos I., Gazetas G., Loli M., Apostolou M, N. Gerolymos, (2010a), "Soil Failure can be used for Seismic Protection of Structures", *Bulletin of Earthquake Engineering*, Vol. 8, pp. 309–326.

Yim, S.C. & Chopra, A.K., (1985), "Simplified earthquake analysis of structures with foundation uplift", *Journal of Structural Engineering* (ASCE), Vol. 111(4), pp. 906–930.

Nakaki, D.K., & Hart, G.C. (1987), "Uplifting response of structures subjected to earthquake motions", Report No. 2.1-3, U.S.–Japan Coordinated Program for Masonry Building Research.

Chen, X. L., & Lai, Y. M., (2003), "Seismic response of bridge piers on elastic-plastic Winkler foundation allowed to uplift", *Journal of Sound and Vibrations*, Vol. 266(5), pp. 957–965.

Houlsby G. T., Amorosi A., & Rojas E., (2005), "Elastic moduli of soils dependent on pressure: a hyperelastic formulation", *Geotechnique*, Vo 55(5), pp. 383 –392.

Allotey, N., & Naggar, MHE., (2003), "Analytical moment–rotation curves for rigid foundations based on a Winkler model", *Soil Dynamics and Earthquake Engineering,* Vol. 23, pp. 367–381.

Allotey, N., & Naggar, MHE., (2007), "An investigation into the Winkler modeling of the cyclic response of rigid footings", *Soil Dynamics and Earthquake Engineering,* Vol. 28, pp. 44–57.

Raychowdhury, P., & Hutchinson, T.C., (2009), "Performance evaluation of a nonlinear Winkler-based shallow foundation model using centrifuge test results", *Earthquake Engineering and Structural Dynamics*, Vol. 38, pp. 679-698.

Nova, R., & Montrasio, L., (1991), "Settlement of shallow foundations on sand", G*eotechnique*, Vol. 41(2), pp. 243-256.

Pedretti, S, (1998), "*Non-linear seismic soil-foundation interaction: analysis and modeling methods*", PhD Thesis, Politechnico di Milano.

Le Pape, Y., & Sieffert, JP., (2001), "Application of thermodynamics to the global modeling of shallow foundations on frictional material". *International Journal for Numerical and Analytical Methods in Geomechanics*, Vol. 25, pp. 1377-1408.

Crémer, C., Pecker, A., & Davenne, L., (2001), "Cyclic macro-element for soil–structure interaction: material and geometrical nonlinearities", *International Journal for Numerical and Analytical methods in Geomechanics*; Vol. 25(12), pp. 1257–1284.

Grange, S., Kotronis, P., & Mazars, J., (2008), "A macro-element for the circular foundation to simulate 3D soil-structure interaction", *International Journal for Numerical and Analytical Methods in Geomechanics*, Vol. 32.

Chatzigogos, C.T., Pecker, A., & Salençon J., (2009), "Macroelement modeling of shallow foundations", *Soil Dynamics and Earthquake Engineering*, Vol. 29 (5), pp. 765-781

Chatzigogos, C.T., Figini, R., & Pecker, A. and J. Salençon, (2010), "A macroelement formulation for shallow foundations on cohesive and frictional soils", *International Journal for Numerical and Analytical Methods in Geomechanics*

Anastasopoulos I. Gelagoti F., Kourkoulis R., Gazetas G., (2011), "Simplified Constitutive Model for Simulation of Cyclic Response of Shallow Foundations : Validation against Laboratory Tests", *Journal of Geotechnical and Geoenvironmetal Engineering*, ASCE (*in print).*

Gouvernec S., (2007), "Shape effects on the capacity of rectangular footings under general loading", *Geotechique*, 57, No. 8, 637-646.

Taiebat, H. A. & Carter, J. P., (2000), "Numerical studies of the bearing capacity of shallow foundations on cohesive soil subjected to combined loading", *Geotechnique*, 50, No. 4, 409–418.

Butterfield, R. & Gottardi, G, (1995), "Simplifying Transformations for the Analysis of Shallow Foundations on Sand", *Proc. 5th Int. Offshore and Polar Eng Conf.*, The Hague, pp. 534-538.

Tan, F.S., (1990). "*Centrifuge and theoretical modelling of conical footings on sand*" Ph.D. thesis, University of Cambridge.

Faccioli E, Paolucci R, G. Vivero, (2001), "Investigation of seismic soil– footing interaction by large scale cyclic tests and analytical models", *Proc. 4th International Conference on Recent Advances in Geotechnical Earthquake Engineering and Soil Dynamics*, Paper no. SPL-5, San Diego, California.

Gajan, S., Kutter, B.L., Phalen, J. D.,Hutchinson, T. C., and G.R. Martin, (2005), "Centrifuge modeling of load-deformation behavior of rocking shallow foundations", *Soil Dynamics and Earthquake Engineering,* 25, pp. 773–783

Kutter B.L, Martin G., Hutchinson T.C., Harden C., Gajan S., and J.D. Phalen, (2003), "Status report on study of modeling of nonlinear cyclic load–deformation behavior of shallow foundations", University of California, Davis, PEER Workshop.

Kawashima K., Nagai T., and D. Sakellaraki, (2007), "Rocking Seismic Isolation of Bridges Supported by Spread Foundations", *Proc. of 2nd Japan-Greece Workshop on Seismic Design, Observation, and Retrofit of Foundations*, Tokyo, Japan, pp. 254–265.

I. Anastasopoulos, P. Kokkali, A. Tsatsis (2011), *"experimental Investigation of Vertical Load Capacity of Surface Footings"*, Laboratory of Soil Mechanics, National Technical University of Athens.

S. Gouvernec (2004), "*Bearing capacity under combined loading- a study of the effect of shear strength heterogeneity",* 9th Australia New Zealand Conference on Geomechanics, Auckland, New Zealand, 8-11 February 2004.

V. Drosos, T. Georgarakos, M. Loli, I. Anastasopoulos, O. Zarzouras, G. Gazetas, M. ASCE (2010), "*Soil-Foundation-Structure Interaction with mobilization of bearing capacity : An experimental Study on Sand".*

F. Gelagoti, R. Kourkoulis, I. Anastasopoulos and G. Gazetas (2011). "*Rocking Isolation of Frames on Isolated Footings: Design Insights and Limitations".*